PACIFIC EARTHQUAKE ENGINEERING RESEARCH CENTER

Rocking Response and Overturning of Equipment under Horizontal Pulse-Type Motions

Nicos Makris
Yiannis Roussos
University of California, Berkeley

PEER 1998/05
OCT. 1998

Rocking Response and Overturning of Equipment Under Horizontal Pulse-Type Motions

by

Nicos Makris
University of California, Berkeley

Yiannis Roussos
University of California, Berkeley

Report PEER-1998/05
Pacific Earthquake Engineering Research Center
College of Engineering
University of California, Berkeley
October 1998

ABSTRACT

In this report the transient rocking response of electrical equipment subjected to trigonometric pulses and near-source ground motions is investigated in detail. First the rocking response of a rigid block subjected to a half-sine pulse motion is reviewed. It is shown that the solution presented by Housner (1963) for the minimum acceleration amplitude of a half-sine pulse that is needed to overturn a rigid block is incorrect. In reality, under a half-sine pulse, a block overturns during its free vibration regime and not at the instant that the pulse expires, as was assumed by Housner. Within the limits of the linear approximation, the correct conditions for a block to overturn are established and the correct expression that yields the minimum acceleration required to overturn a block is derived. Subsequently, physically realizable cycloidal pulses are introduced and their resemblance to recorded near-source ground motions is illustrated. The study uncovers the coherent component of some near-source acceleration records, and the overturning potential of these motions is examined. The rocking response of rigid blocks subjected to cycloidal pulses and near-source ground motions is computed with a linear and nonlinear formulation. It is found that the toppling of smaller blocks depends not only on the incremental ground velocity but also on the duration of the pulse, whereas the toppling of larger blocks depends mostly on the incremental ground velocity. The kinematic characteristics of recorded near-source ground motions are examined in detail. It is found that the high frequency fluctuations that occasionally override the long duration pulse will overturn a smaller block, whereas a larger block will overturn due to the long duration pulse. A method to determine the cut-off frequency is developed and illustrated through examples. In this light, the rocking response of electrical equipement subjected to near-source ground motions is shown to be quite ordered and predictable.

TABLE OF CONTENTS

LIST OF FIGURES

LIST OF TABLES

ACKNOWLEDGMENTS

This work is supported by the Pacific Gas and Electric Company under Grant PG&E-UCB-9 to the Pacific Earthquake Engineering Center. The valuable input and comments of Dr. Norm Abrahamson, Mr. Eric Fujisaki, and Mr. Henry Ho are greatly appreciated.

CHAPTER 1
INTRODUCTION

During strong ground shaking, a variety of rigid structures such as concrete radiation shields, electrical transformers, and other heavy equipment might slide or set up a rocking motion that results in substantial damage. Early studies on the dynamic response of a rigid block supported on a base undergoing horizontal motion were presented by Housner (1963). In that study, the base acceleration was represented by a rectangular or a half-sine pulse, and expressions were derived for the minimum acceleration required to overturn the block. Using an energy approach, he presented an approximate analysis of the dynamics of a rigid block subjected to a white noise excitation, uncovering a scale effect that explained why the larger of two geometrically similar blocks can survive the excitation whereas the smaller block may topple. He also indicated that toppling of a given block depends on the product of the acceleration amplitude of the pulse by its duration. This fundamental finding that toppling of a block depends on the incremental velocity (area under the acceleration pulse) and not merely on the peak ground acceleration (West's formula, Milne 1885, Hogan 1989) did not receive the attention it deserves. Yim et al. (1980) adopted a probabilistic approach and conducted a numerical study using artificially generated ground motions to show that the rocking response of a block is sensitive to system parameters. Their simulation procedure consisted of generating samples of Gaussian white noise that was multiplied by an intensity function of time and subsequently filtered through a second-order linear filter to impart a smooth transfer function with a maximum at 2.5 Hz. The white-noise type motions used by Yim et al. do not contain any coherent component, and the overturning of the block is the result of a rapid succession of small random impulses (areas under the spikes of the artificially generated high frequency acceleration histories). It is partly because of the very nature of the ground motions used that the results exhibit such a high sensitivity to system parameters.

Experimental and analytical studies on the same problem have been reported by Aslam et al. (1980). Their study concludes that, in general, the rocking response of blocks subjected to earthquake motion is in line with the conclusions derived from single pulse excitations. However, when artificially generated motions were used, the rocking response showed high sensitivity to the system parameters.

The rocking response of blocks subjected to harmonic steady-state loading was studied in detail by Spanos and Koh (1984) who identified “safe” and “unsafe” regions and developed analytical methods for determining the fundamental and subharmonic modes of the system. Their study was extended by Hogan (1989, 1990) who further elucidated the mathematical structure of the problem by introducing the concepts of orbital stability and Poincaré section. Hogan (1989) showed that there is a minimum value of the forcing amplitude, dependent on frequency, below which the block asymptotic motion ceases. Perhaps Hogan’s most relevant finding to earthquake engineering is that the domain of maximum transients of his solutions appears relatively ordered and possesses a high degree of predictability despite the unpredictability that is present in the asymptotic part of the solutions. The steady-state rocking response of rigid blocks was also studied analytically and experimentally by Tso and Wong (1989 a, b). While their theoretical study was not as in-depth as the one presented by Hogan, their experimental work provided valuable support to theoretical findings. Other related studies are referenced in the above-mentioned papers.

While the early work of Yim et al. (1980) used artificially generated white-noise-type motions, and the work of Spanos and Koh (1984), Hogan (1989, 1990), and Tso and Wong (1989) used long-duration harmonic motions, our attention in this report is redirected to pulse-type motions which are found to be good representations of near-source ground motions (Campillo et al. 1989, Iwan and Chen 1994).

During a seismic event, the ground movement in the near-fault region is primarily the result of waves that are moving in the same direction as the fault rupture, thereby crowding together to produce a long-duration pulse. Near-source ground motions have distinguishable long duration pulses. In some cases, coherent pulses are distinguishable not only in the displacement and velocity histories but also in the acceleration history in which the peak acceleration reaches usually moderate values. In other cases, acceleration records contain high spikes and resemble the traditional random-like motions, but their velocity and displacement history uncover a coherent long-period pulse with some high frequency fluctuations that override along. What makes these motions particularly destructive to some engineering structures is not their peak acceleration but the area under the long duration acceleration pulse which represents the incremental velocity that the above ground mass has to reach (Anderson and Bertero 1986). In this report, we built on

Housner's (1963) pioneering work to investigate the overturning potential of a near-source ground motion. It is shown that the toppling of smaller blocks depends not only on the incremental ground velocity (area under the acceleration pulse), but also on the duration of the pulse, whereas the toppling of larger blocks tends to depend solely on the incremental ground velocity. Accordingly, a smaller block might overturn due to the high-frequency fluctuations that override the long duration pulse, whereas a larger block will overturn due to the long duration pulse.

The study of the rocking response of rigid blocks to near-source ground motions was motivated by the proximity of major urban areas and their power plants to active faults. For instance, the San Andreas fault runs 10 km west of San Francisco, California; much of Oakland, California is within 10 km of the Hayward fault, and a large part of the greater Los Angeles metropolitan region in Southern California, lies over buried thrust faults capable of generating large earthquakes such as the January 17, 1994 Northridge earthquake. The city of Kobe, Japan was devastated by the January 17, 1995 Hyogo-ken Nanbu earthquake, which generated unusually large pulses.

In Chapter 2, the equations of motion with their analytical solutions at the linear limit are presented. We commence our analysis by revisiting the rocking response of a rigid block subjected to a half-sine pulse. It is shown analytically in Chapter 3 that the solution presented by Housner (1963) for the minimum overturning acceleration amplitude is incorrect. This is because, under a half sine pulse, a block overturns during its free vibration response and not at the instant that the pulse expires. Within the limits of the linear approximation, the correct conditions for a block to overturn are established, and the correct expression that yields the minimum acceleration to overturn a block is derived. It is shown that the minimum overturning velocity amplitude depends on the slenderness of the block, the size of the block, and the duration of the pulse.

In Chapter 4 , selected near-source ground motions are presented, and their resemblance to physically realizable cycloidal pulses is shown. A type-A cycloidal pulse approximates a forward pulse, a type-B cycloidal pulse approximates a forward-and-back pulse, whereas a type-C_n pulse approximates a recorded motion that exhibits n main cycles in its displacement history. The velocity histories of all type-A, type-B, and type-C_n pulses are differentiable signals that result in finite acceleration values. Chapters 5, 6, and 7 study the rocking response of a free standing block subjected to type-A, type-B, and type-C_n pulses respectively. In Chapter 8, the effects on the nonlinear nature of the rocking motion are illustrated, and the accuracy of the nonlinear numerical algorithm is validated. In Chapter 9, the rocking response of free-standing blocks subjected to near-source ground motions is examined in detail, showing that smaller blocks overturn due to short duration pulses with high acceleration, whereas larger blocks that survive these pulses will overturn from larger duration pulses with smaller peak acceleration. Chapter 10 is devoted to a summary of the findings and conclusions.

CHAPTER 2
PROBLEM DEFINITION AND EQUATIONS OF MOTION

Consider the model shown in Figure 1, which can oscillate about the centers of rotation O and O' when it is set to rocking. Its center of gravity coincides with the geometric center, which is at a distance R from any corner. The angle α of the block is given by $\tan(\alpha) = b/h$. Depending on the value of the ground acceleration and the coefficient of friction, μ, the block may translate with the ground, enter a rocking motion or a sliding motion. A necessary condition for the block to enter a rocking motion is $\mu > b/h$ (Aslam et al. 1980, Scalia and Sumbatyan 1996). The possibility for a block to slide during the rocking motion has been investigated by Zhu and Soong (1997), and Pompei et al. (1998). In this study, it is assumed that the coefficient of friction between the block and its base is sufficiently large to prevent sliding at any instant in the rocking motion. Under a positive horizontal ground acceleration, $\ddot{u}_g$, the block will initially rotate with a negative rotation, $\theta<0$, and, if it does not overturn, it will eventually assume a positive rotation and so forth. Assuming zero vertical base acceleration ($\ddot{v}_g(t) = 0$), the equations of motion are

$$I_o\ddot{\theta} + mgR\sin(-\alpha-\theta) = -m\ddot{u}_gR\cos(-\alpha-\theta)\ ,\ \theta<0, \tag{2.1}$$

and

$$I_o\ddot{\theta} + mg\sin(\alpha-\theta) = -m\ddot{u}_gR\cos(\alpha-\theta)\ ,\ \theta>0. \tag{2.2}$$

For rectangular blocks, $I_o = \frac{4}{3}mR^2$, equations (2.1) and (2.2) can be expressed in the compact form

$$\ddot{\theta}(t) = -p^2\left\{\sin(\alpha\,\mathrm{sgn}[\theta(t)]-\theta(t)) + \frac{\ddot{u}_g}{g}\cos(\alpha\,\mathrm{sgn}[\theta(t)]-\theta(t))\right\}, \tag{2.3}$$

where $p = \sqrt{\frac{3g}{4R}}$ is a quantity with units in rad/sec. The larger the block is (larger R), the smaller p is. The oscillation frequency of a rigid block under free vibration is not constant, since it strongly depends on the vibration amplitude (Housner, 1963). Nevertheless, the quantity p is a measure of the dynamic characteristics of the block. For an electrical transformer, $p \approx 2rad/s$,

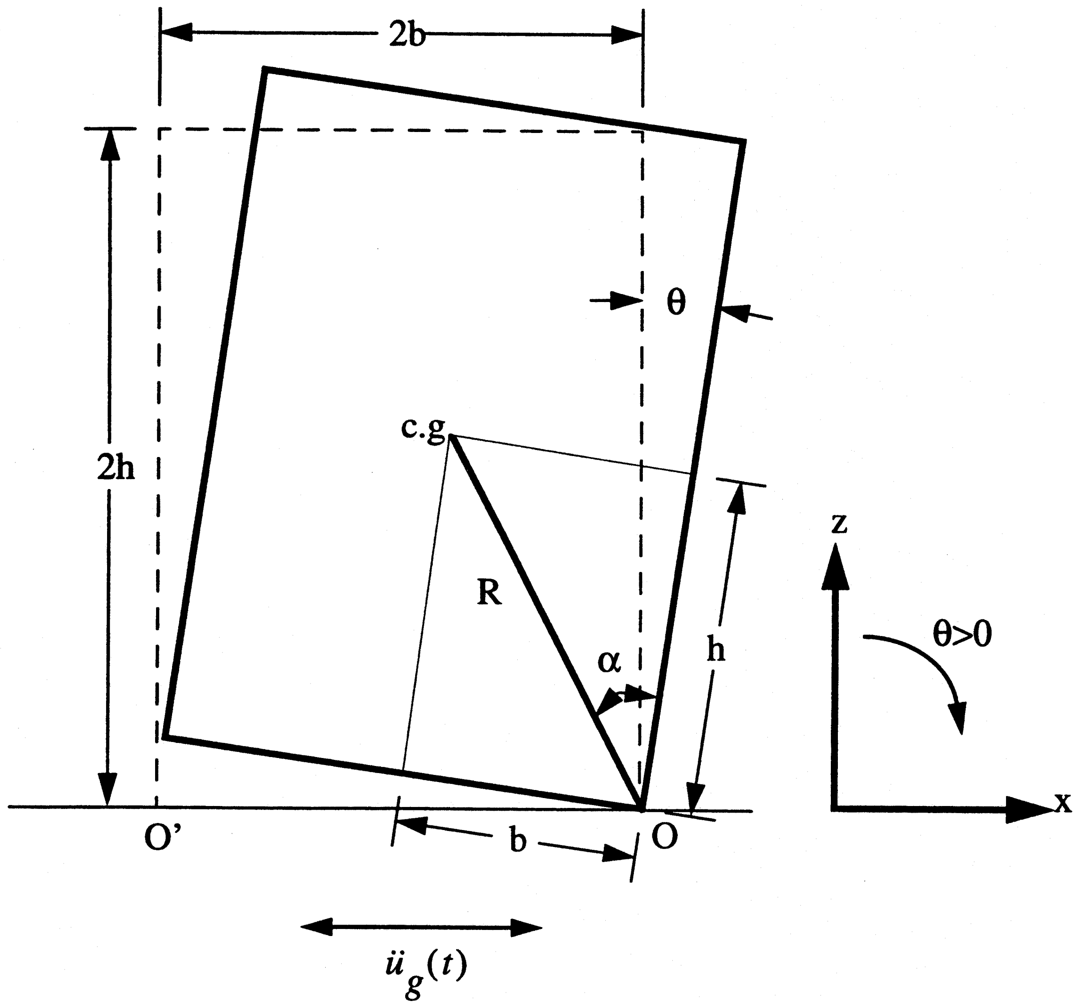

Figure 1: Schematic of rocking block.

and for a household brick, $p \approx 8 rad/s$. Table 2.1 summarizes approximate geometric and dynamic characteristics of electrical equipement that have been subjected to strong rocking motion during earthquake shaking (Fujisaki 1998).

TABLE 2.1. Approximate geometric characteristics and estimated values of the frequency parameter, p, of electrical equipement.

Equipment	b(ft)	h(ft)	R(ft)	α(rad)	p(rad/s)
E1	3.0	6.0	6.71	0.4636	1.90
E2*	1.5	2.5	2.92	0.5404	2.32
E3	8.0	20	21.54	0.3805	1.06
E4	1.5	3.0	3.35	0.4636	2.68
E5	1.75	4.5	4.83	0.3709	2.24
E6	1.25	4.25	4.43	0.2860	2.33
E7*	1.5	2.5	2.92	0.5404	2.32
E8	1.0	3.5	3.64	0.2783	2.58
E9	1.75	2.75	3.26	0.5667	2.21
E10*	1.75	2.75	3.26	0.5667	2.21
E11*	2.5	4.5	5.15	0.5070	1.73

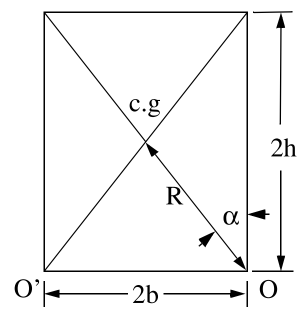

* Cylindrical shapes

When the block is rocking, it is assumed that the rotation continues smoothly from point O to O'. Conservation of momentum about point O' just before the impact and right after the impact gives

$$I_o\dot{\theta}_1 - m\dot{\theta}_1 2bR\sin(\alpha) = I_o\dot{\theta}_2 , \tag{2.4}$$

where $\dot{\theta}_1$ is the angular velocity just prior to the impact, and $\dot{\theta}_2$ is the angular velocity right after the impact. The ratio of kinetic energy after and before the impact is

$$r = \frac{\dot{\theta}_2^2}{\dot{\theta}_1^2} , \tag{2.5}$$

which means that the angular velocity after the impact is only $\sqrt{r}$ times the velocity before the impact. Substitution of (2.5) into (2.4) gives

$$r = \left[1 - \frac{3}{2}\sin^2\alpha\right]^2 . \tag{2.6}$$

The value of the coefficient of restitution given by (2.6) is the maximum value of r under which a block with slenderness α will undergo rocking motion. If additional energy is lost due to interface mechanisms, the value of the true coefficient of restitution, r, will be less than the one computed from (2.6). In this study, the entire analysis is conducted using the maximum value of the coefficient of restitution given by (2.6).

Equations (2.1) and (2.2) are well known in the literature (for example, Yim et al. 1980, Spanos and Koh 1984, Hogan 1989). They are valid for arbitrary values of the block angle α. For tall slender blocks, the angle $\alpha = \tan^{-1}(b/h)$ is relatively small and equations (2.1) and (2.2) can be linearized. Closed form solutions of the linearized equations for harmonic excitation have been presented by Housner (1963) for positive rotations only $(\theta > 0)$, and by Hogan (1989) for positive and negative rotations. Herein, the solution of the linearized equations is derived for a sinusoidal ground motion for both positive and negative rotations in order to revisit the overturning conditions due to a half-sine pulse that were postulated by Housner and to examine the rocking behavior of rigid blocks subjected to cycloidal pulses. Within the limits of the linear approximation and for a ground acceleration

$$\ddot{u}_g(t) = a_p \sin(\omega_p t + \psi) , \tag{2.7}$$

equations (2.1) and (2.2) become

$$\ddot{\theta}(t) - p^2\theta(t) = -\frac{a_p}{g}p^2\sin(\omega_p t + \psi) + p^2\alpha \ , \ \theta<0 \tag{2.8}$$

and

$$\ddot{\theta}(t) - p^2\theta(t) = -\frac{a_p}{g}p^2\sin(\omega_p t + \psi) - p^2\alpha \ , \ \theta>0, \tag{2.9}$$

where $\psi = \sin^{-1}(\alpha g/a_p)$ is the phase when rocking initiates. Assuming a zero initial rotation, the integration of (2.8) and (2.9) gives

$$\theta(t) = A_1 \sinh(pt) + A_2 \cosh(pt) - \alpha + \frac{1}{1+\frac{\omega_p^2}{p^2}} \frac{a_p}{g} \sin(\omega_p t + \psi) \ , \ \theta<0 \tag{2.10}$$

and

$$\theta(t) = A_3 \sinh(pt) + A_4 \cosh(pt) + \alpha + \frac{1}{1+\frac{\omega_p^2}{p^2}} \frac{a_p}{g} \sin(\omega_p t + \psi) \ , \ \theta>0, \tag{2.11}$$

where

$$A_1 = A_3 = \frac{\dot{\theta}_0}{p} - \frac{\omega_p/p}{1+\omega_p^2/p^2} \frac{a_p}{g} \cos(\psi) = \frac{\dot{\theta}_0}{p} - \alpha \frac{\omega_p/p}{1+\omega_p^2/p^2} \frac{\cos(\psi)}{\sin(\psi)} \ , \tag{2.12}$$

$$A_2 = \theta_0 + \alpha - \frac{1}{1+\omega_p^2/p^2} \frac{a_p}{g} \sin(\psi) = \theta_0 + \alpha - \frac{\alpha}{1+\omega_p^2/p^2} \ , \tag{2.13}$$

$$A_4 = \theta_0 - \alpha - \frac{1}{1+\omega_p^2/p^2} \frac{a_p}{g} \sin(\psi) = \theta_0 - \alpha - \frac{\alpha}{1+\omega_p^2/p^2} \ . \tag{2.14}$$

The time histories for the angular velocities are directly obtained from the time derivatives of (2.10) and (2.11)

$$\dot{\theta}(t) = pA_1 \cosh(pt) + pA_2 \sinh(pt) + \frac{\omega_p}{1+\frac{\omega_p^2}{p^2}} \frac{a_p}{g} \cos(\omega_p t + \psi) \ , \ \theta<0 \tag{2.15}$$

and

$$\dot{\theta}(t) = pA_3 \cosh(pt) + pA_4 \sinh(pt) + \frac{\omega_p}{1+\frac{\omega_p^2}{p^2}} \frac{a_p}{g} \cos(\omega_p t + \psi) \ , \ \theta>0. \tag{2.16}$$

The solution presented by Housner (1963) is a special case of the solution given by (2.10) to (2.14). Assuming zero initial rotation and zero initial angular velocity $(\theta(0)) = \dot{\theta}(0) = 0)$, the substitution of (2.12) and (2.13) into (2.10) gives

$$-\theta(t) = \alpha + \frac{\alpha}{1+\frac{\omega_p^2}{p^2}}\left[\frac{\omega_p}{p}\frac{a_p}{\alpha g}\cos\psi\sin\psi - \frac{\omega_p^2}{p^2}\cosh(pt) - \frac{a_p}{\alpha g}\sin(\omega_p t + \psi)\right] . \tag{2.17}$$

Recalling that $\sin\psi = \alpha g / a_p$, equation (2.17) takes the form

$$-\theta(t) = \alpha + \frac{\alpha}{1+\frac{\omega_p^2}{p^2}}\left[\frac{\omega_p}{p}\frac{\cos\psi}{\sin\psi}\sinh(pt) - \frac{\omega_p^2}{p^2}\cosh(pt) - \frac{\sin(\omega_p t + \psi)}{\sin\psi}\right] , \tag{2.18}$$

which is the solution reported by Housner (equation (10) in his paper). The minus sign on the left hand side of (2.18) is because we considered that the ground moves with a positive sine acceleration, and therefore the block initially rotates with a negative angle $\theta(t) < 0$.

CHAPTER 3
RESPONSE TO A HALF-SINE PULSE

The analytical solutions given by (2.10), (2.11), (2.15), and (2.16) can be used to compute the linear rocking response and the minimum acceleration amplitude of any sinusoidal excitation with finite duration that is needed to overturn a block. A solution for the minimum acceleration amplitude of a half-sine pulse that is needed to overturn a block was presented by Housner (1963). Unfortunately, the solution presented in that pioneering work and subsequently presented in later papers (Yim et al. 1980, among others) is incorrect. In this chapter this flaw is rectified by establishing the conditions necessary for a block to overturn.

In his seminal paper, Housner postulated that the condition for overturning is that the angle of rotation, θ, is equal to the angle α of the block at time $t = (\pi - \psi)/\omega_p$, which is the time that the half-sine pulse expires. Based on this forced postulate, he derived a simple expression that provides the minimum acceleration amplitude required to overturn the block.

In reality, under the minimum acceleration amplitude, the block will overturn during its free vibration regime. This can be easily found by examining the free vibration response where the homogeneous part of the solution is expressed by (2.10) and (2.11) with $a_p = 0$. In the homogeneous solution, the initial rotation θ_0 and initial angular velocity $\dot{\theta}_0$ in the integration constants, A_1 and A_2, are the rotation and angular velocity of the block at the instant when the sinusoidal excitation expires. Figure 2 plots the response of a rigid block with dimensions b=0.2 m and h=0.6 m subjected to a half-sine pulse excitation with duration 0.5 sec and excitation frequency $\omega_p = 2\pi$. On the left of Figure 2 the amplitude of the acceleration pulse is $a_g = 5.430$ m/sec^2 (0.5535g) and the block does not overturn, whereas on the right of Figure 2, $a_g = 5.440$ m/sec^2 (0.5545g) and the block overturns. The solid line is the analytical solution presented in Chapter 2, and the dashed line is the result of the numerical solution of the linearized equations of motion presented in Chapter 8. Figure 2 illustrates that the overturning of the block happens much later than the time Housner had considered i.e., the end of the excitation pulse. Under the ideal condition that the block is being subjected to the exact value of the minimum acceleration needed to overturn it, the time when overturning occurs is infinitely large.

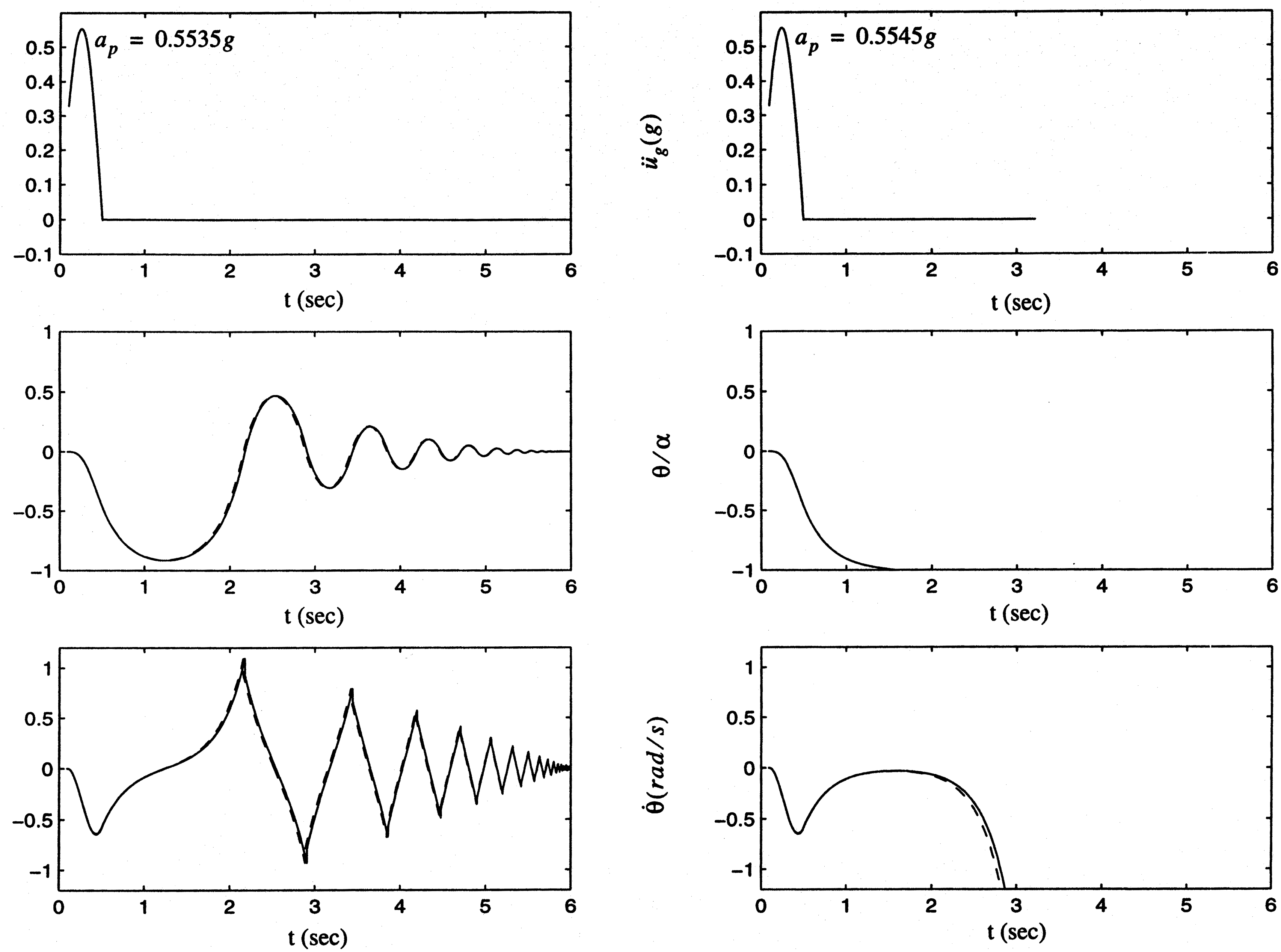

Figure 2: Rotation and angular velocity time histories of a rigid block (b=0.2 m, h=0.6 m) subjected to a half-sine pulse excitation. Left: no overturning. Right: overturning. Solid line: analytical solution. Dashed line: numerical solution with linear formulation

With b=0.2m and h=0.6m, the slenderness angle $\alpha = \tan^{-1}(b/h) = 0.3217$ rad and p=3.411 rad/sec. For $\omega_p = 6.28$ rad/sec, $\omega_p/p = 1.84$ and according to Housner's calculation, the minimum acceleration amplitude that will overturn the block is $a_g = \alpha g\sqrt{1+(\omega_p/p)^2} \approx 0.673g$, whereas Figure 2 shows that an acceleration amplitude of $a_g = 0.5545g$ is sufficient to overturn the block. Consequently, within the limits of the linear formulation, the minimum acceleration values reported by Housner and later by Yim et al. (1980) are unconservative.

The time that the overturning occurs is very sensitive to the value of the acceleration amplitude. Figure 3 shows the computed response for two different acceleration amplitudes in the vicinity of the critical acceleration. It is shown that a slight increase in the acceleration has a significant effect on the time history response. The more the acceleration amplitude approaches the critical overturning acceleration, the more the block will delay before re-centering, and, for the exact value of the critical acceleration, the block will theoretically spend an infinitely long time deciding whether it should re-center or overturn. This observation indicates that the limit state condition for overturning is that the time when overturning occurs can be arbitrarily large.

The overturning condition of the block is established in Figure 2, which suggests that the block experiences the maximum rotation during the free vibration regime. Since the angle of rotation at the end of the excitation pulse is negative, the equation of motion during the free vibration regime that immediately follows is

$$\theta(t) = A_1 \sinh(pt) + A_2 \cosh(pt) , \tag{3.1}$$

where A_1 and A_2 are integration constants that depend on the rotation and angular velocity of the block at the end of the excitation pulse and are given by

$$A_1 = \frac{\dot{\theta}_0}{p} \ , \ A_2 = \theta_0 + \alpha . \tag{3.2}$$

During this free vibration regime that immediately follows the forced vibration regime, the block will not overturn as long as the angular velocity decreases in magnitude monotonically, reaches zero, and then increases while the block rotates back to the equilibrium position. How-

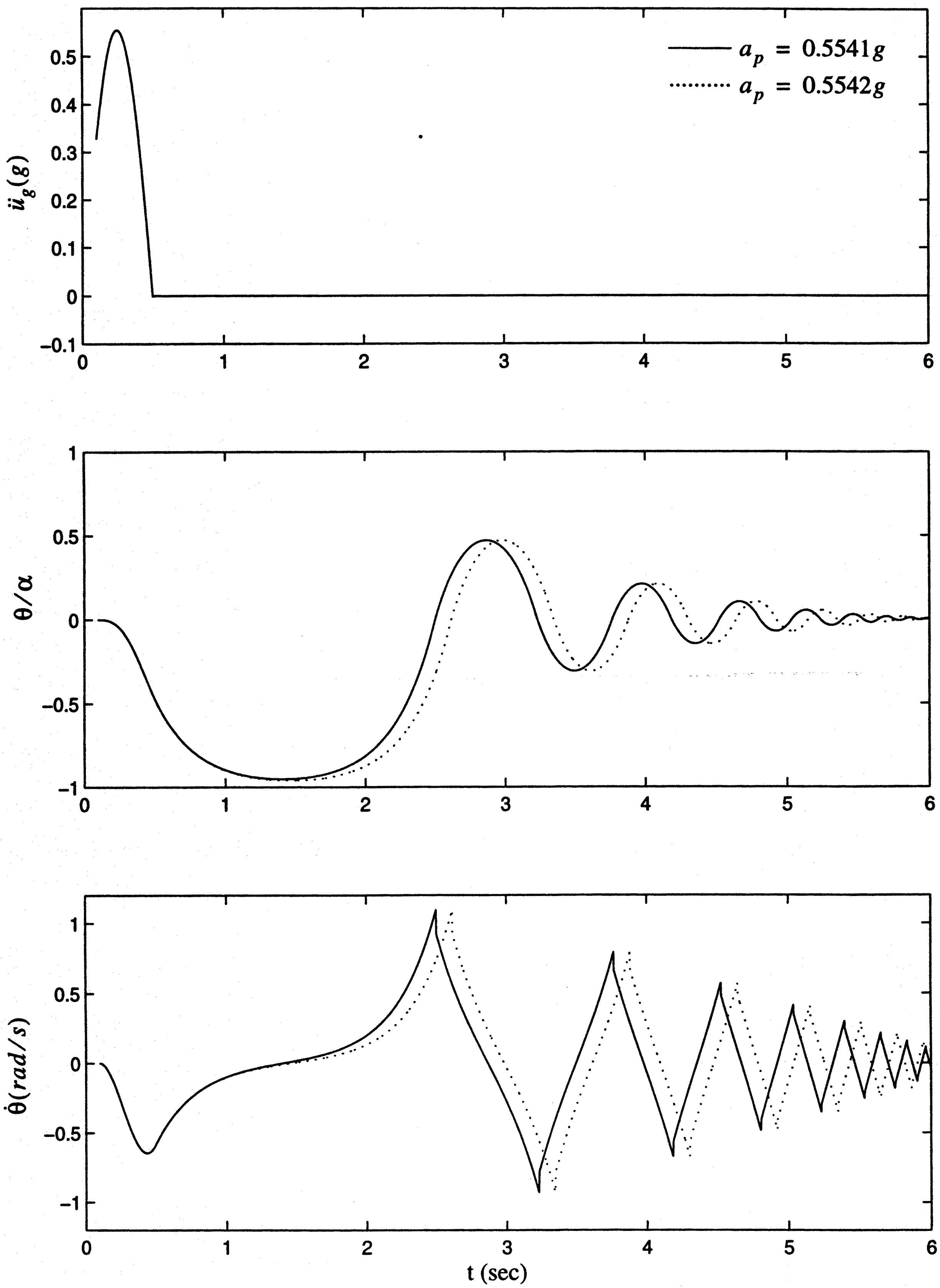

Figure 3: Rotation and angular velocity time histories of a rigid block (b=0.2 m, h=0.6 m) subjected to a half-sine pulse excitation with near-critical acceleration amplitude. A small variation in acceleration amplitude creates a significant variation in the response.

ever, if the velocity does not reach zero, but instead reaches an extremum, the block will overturn. Accordingly, the block overturns when

$$\ddot{\theta}(t) = A_1 p^2 \sinh(pt) + p^2 A_2 \cosh(pt) = 0 \tag{3.3}$$

which gives

$$\tanh(pt) = -\frac{A_2}{A_1}. \tag{3.4}$$

Our previous analysis uncovered that, under the critical acceleration, the time when overturning occurs is large enough so that tanh(pt)=1, and the condition for overturning reduces to

$$A_1 + A_2 = 0. \tag{3.5}$$

The computation of A_1 and A_2 (see equations (2.12) and (2.13)) involves the evaluation of θ_0 and $\dot{\theta}_0$ at the beginning of the free vibration regime, which occurs at time $t = (\pi - \psi)/\omega_p$. Consequently, θ_0 and $\dot{\theta}_0$ are computed from equation (2.18) and its derivatives at time $t = (\pi - \psi)/\omega_p$. This gives

$$\theta_0 = -\alpha - \frac{\alpha}{1 + \frac{\omega_p^2}{p^2}} \frac{\omega_p}{p}\left[\frac{\cos\psi}{\sin\psi}\sinh\left[\frac{p}{\omega_p}(\pi - \psi)\right] - \frac{\omega_p}{p}\cosh\left[\frac{p}{\omega_p}(\pi - \psi)\right]\right], \tag{3.6}$$

$$\dot{\theta}_0 = \frac{-\alpha p}{1 + \frac{\omega_p^2}{p^2}} \frac{\omega_p}{p}\left[\frac{\cos\psi}{\sin\psi}\cosh\left[\frac{p}{\omega_p}(\pi - \psi)\right] - \frac{\omega_p}{p}\sinh\left[\frac{p}{\omega_p}(\pi - \psi)\right] + \frac{1}{\sin\psi}\right]. \tag{3.7}$$

With the substitution of the expressions (3.6) and (3.7) into (2.12) and (2.13), equation (3.5) takes the form

$$\begin{aligned} &\cos\psi\cosh\left[\frac{p}{\omega_p}(\pi - \psi)\right] - \frac{\omega_p}{p}\sin\psi\sinh\left[\frac{p}{\omega_p}(\pi - \psi)\right] + 1 \\ &+ \cos\psi\sinh\left[\frac{p}{\omega_p}(\pi - \psi)\right] - \frac{\omega_p}{p}\sin\psi\cosh\left[\frac{p}{\omega_p}(\pi - \psi)\right] = 0 \end{aligned} \tag{3.8}$$

Equation (3.8) is the condition for overturning. The solution of this transcendental equation gives the value of ψ for which the acceleration $a_{po} = \alpha g/(\sin\psi)$ is the minimum acceleration needed to overturn the block. Figure 4 (top) plots with a solid line the solution of (3.8) as a function of ω_p/p, and is compared with the unconservative solution presented by Housner (1963) (dotted line).

The points shown in Figure 4 (top) are the numerical solutions for different values of the block slenderness obtained with a nonlinear formulation that is presented in Chapter 8. Figure 4 (top) also illustrates that, in the range $0 \le \omega_p/p \le 4$, the minimum overturning acceleration amplitude is a nearly linear function of ω_p/p. A dependable approximation of the correct solution is

$$\frac{a_{po}}{\alpha g} \approx 1 + \frac{1}{2}\frac{\omega_p}{p}. \tag{3.9}$$

At the end of the half-sine pulse, the ground has reached the constant velocity $v_p = 2a_p/\omega_p$. For a rectangular block, $p = \sqrt{3g/(4R)}$, equation (3.9) offers a dependable approximation for the minimum overturning velocity amplitudes

$$v_{po} = \frac{a_{po}T_p}{\pi} \approx 2\alpha\left(\frac{T_p g}{2\pi} + \sqrt{\frac{Rg}{3}}\right). \tag{3.10}$$

The results of the approximate expression given by (3.10) are shown in Figure 4 (bottom) next to the exact linear solution (solid line), the numerical solution (points), and the unconservative solution presented by Housner (1963). Equation (3.10) shows that, for $\omega_p/p < 3$, the minimum overturning velocity amplitude depends not only on the slenderness, α, and the size, R, but also on the duration of the pulse. Consequently, if one considers two different half-sine acceleration pulses with the same product a_pT_p, the short-period pulse with the larger acceleration amplitude is more capable of overturning a block than the longer period pulse with the smaller acceleration amplitude.

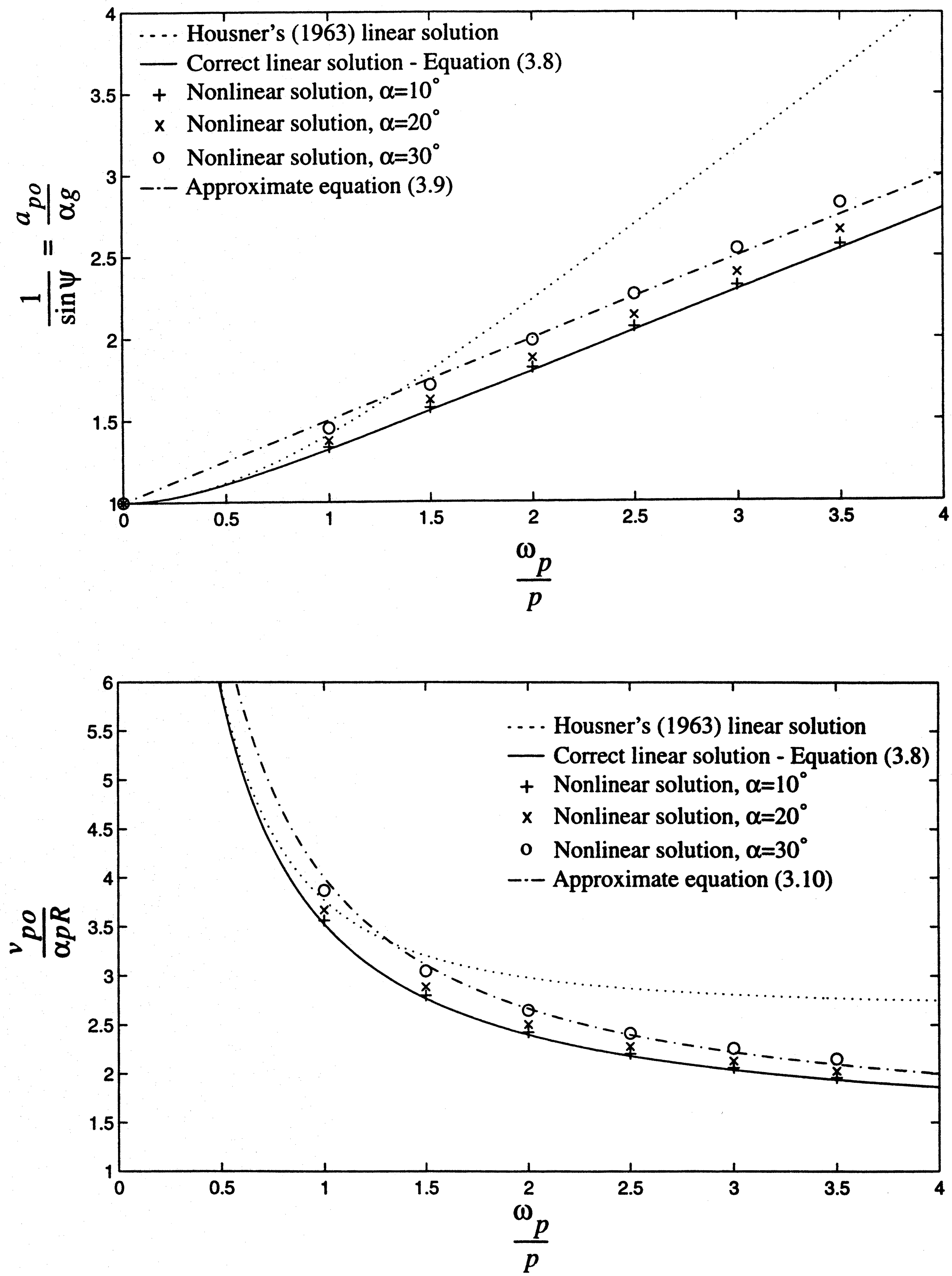

Figure 4: Top: Spectrum of the minimum acceleration amplitude, a_{po}, of a half-sine pulse needed to overturn a free standing block. Bottom: Spectrum of the minimum velocity amplitude, v_{po}, of a half-sine pulse needed to overturn a free standing block.

CHAPTER 4
CLOSED FORM APPROXIMATION OF NEAR-SOURCE GROUND MOTIONS

During the last two decades, an ever increasing database of recorded earthquakes has demonstrated that the dynamic characteristics of the ground near the faults of major earthquakes have distinguishable long duration pulses. Near-source ground motions contain large displacement pulses, say one or two coherent pulses from 0.5 m to more than 1.5 m with peak velocities of 0.5 m/s or higher. Their duration is usually between one to three seconds, but it can be as long as 6 s. A typical value of the frequency, p, for an electrical transformer is $p \approx 2$, therefore the low frequency range $\omega_p / p \leq 3.0$ is of interest. Of particular interest are the forward motions, the forward-and-back motions, motions that exhibit one main cycle in their displacement history, and motions that exhibit two main cycles in their displacement histories.

Figure 5 (left) shows the East-West components of the acceleration, velocity and displacement histories of the September 19th, 1985 Michoacan earthquake recorded at the Caleta de Campos station (Anderson et al. 1986). The motion resulted in a forward displacement of the order of 0.4 m. The coherent long duration pulse responsible for most of this displacement can also be distinguished in the velocity history, whereas the acceleration history is crowded with high frequency spikes. Figure 5 (right) plots the acceleration, velocity, and displacement histories of a type-A cycloidal pulse given by (Jacobsen and Ayre 1958, Makris 1997)

$$\ddot{u}_g(t) = \omega_p \frac{v_p}{2} \sin(\omega_p t), \ 0 \leq t \leq T_p, \tag{4.1}$$

$$\dot{u}_g(t) = \frac{v_p}{2} - \frac{v_p}{2} \cos(\omega_p t), \ 0 \leq t \leq T_p, \tag{4.2}$$

$$u_g(t) = \frac{v_p}{2} t - \frac{v_p}{2\omega_p} \sin(\omega_p t), \ 0 \leq t \leq T_p. \tag{4.3}$$

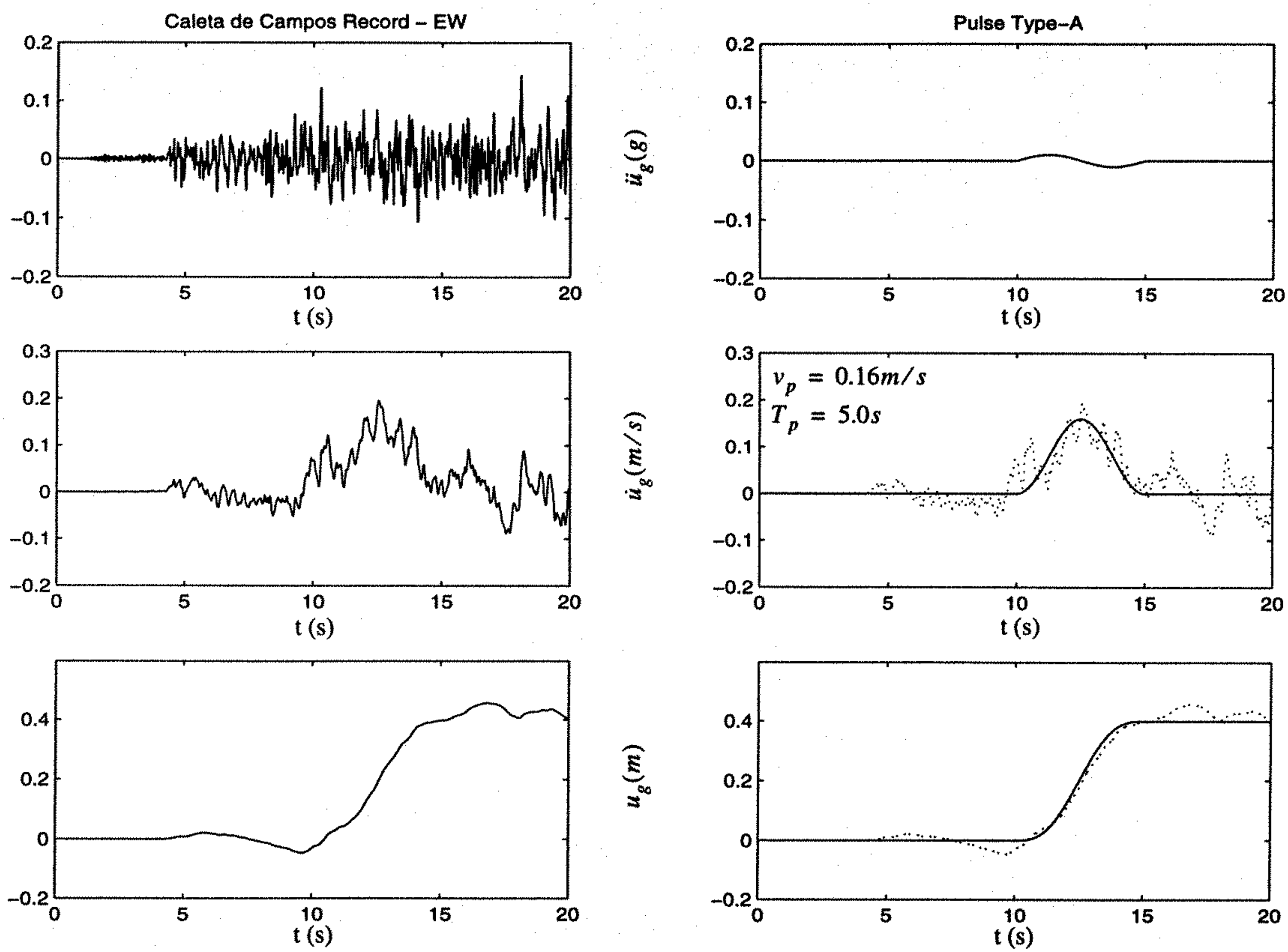

Figure 5: Fault normal components of the acceleration, velocity, and displacement time histories recorded at the Caleta de Campos station during the September 19th, 1985 Michoacan, earthquake (left), and a cycloidal type-A pulse (right).

In constructing Figure 5 (right), the values of Tp=5.0 sec and V_p=0.16 m/sec were used. These are approximations of the duration and velocity amplitude of the main pulse. Figure 5 indicates that a simple one-sine pulse can capture some of the kinematic characteristics of the motion recorded at the Caleta de Campos station. On the other hand, the resulting acceleration amplitude, $a_p = \omega_p v_p / 2 \approx 0.01 g$, is one order of magnitude smaller than the recorded peak ground acceleration.

Another example of a recorded ground motion that resulted in a forward pulse is the fault parallel motion recorded at the Lucerne Valley station during the June 18th, 1992 Landers earthquake, which is shown on Figure 6 (left). Although the displacement history results in a clean forward pulse, the acceleration history is crowded with high-frequency spikes that reach 0.75 g. On the right of Figure 6, the results of equations (4.1) to (4.3) are shown for the values of T_p=7.0 s and V_p=0.5 m/s, which are approximations of the pulse period and the pulse velocity amplitude of the recorded motion. Again, while the resulting displacement history is in very good agreement with the record, the resulting acceleration amplitude $a_p = \omega_p v_p / 2 = 0.045 g$ is one order of magnitude smaller than the recorded peak ground acceleration.

Figure 7 (left) shows the acceleration, velocity, and displacement histories of the fault-normal motions recorded at the El Centro Station Array #5 during the October 15th, 1979 Imperial Valley earthquake. This motion resulted in a forward-and-back pulse with a 3.2 sec duration. In this case, the coherent long period pulse is distinguishable not only in the displacement and velocity record, but also in the acceleration record. Figure 7 (right) plots the acceleration, velocity, and displacement histories of a type-B cycloidal pulse given by Makris (1997).

$$\ddot{u}_g(t) = \omega_p v_p \cos(\omega_p t), \; 0 \le t \le T_p, \tag{4.4}$$

$$\dot{u}_g(t) = v_p \sin(\omega_p t), \; 0 \le t \le T_p, \tag{4.5}$$

$$u_g(t) = \frac{v_p}{\omega_p} - \frac{v_p}{\omega_p}\cos(\omega_p t), \; 0 \le t \le T_p. \tag{4.6}$$

In constructing Figure 7 (right) the values of T_p=3.2 s and V_p=0.7 m/s were used as approximate values of the pulse period and velocity amplitude of the recorded motions shown on the left.

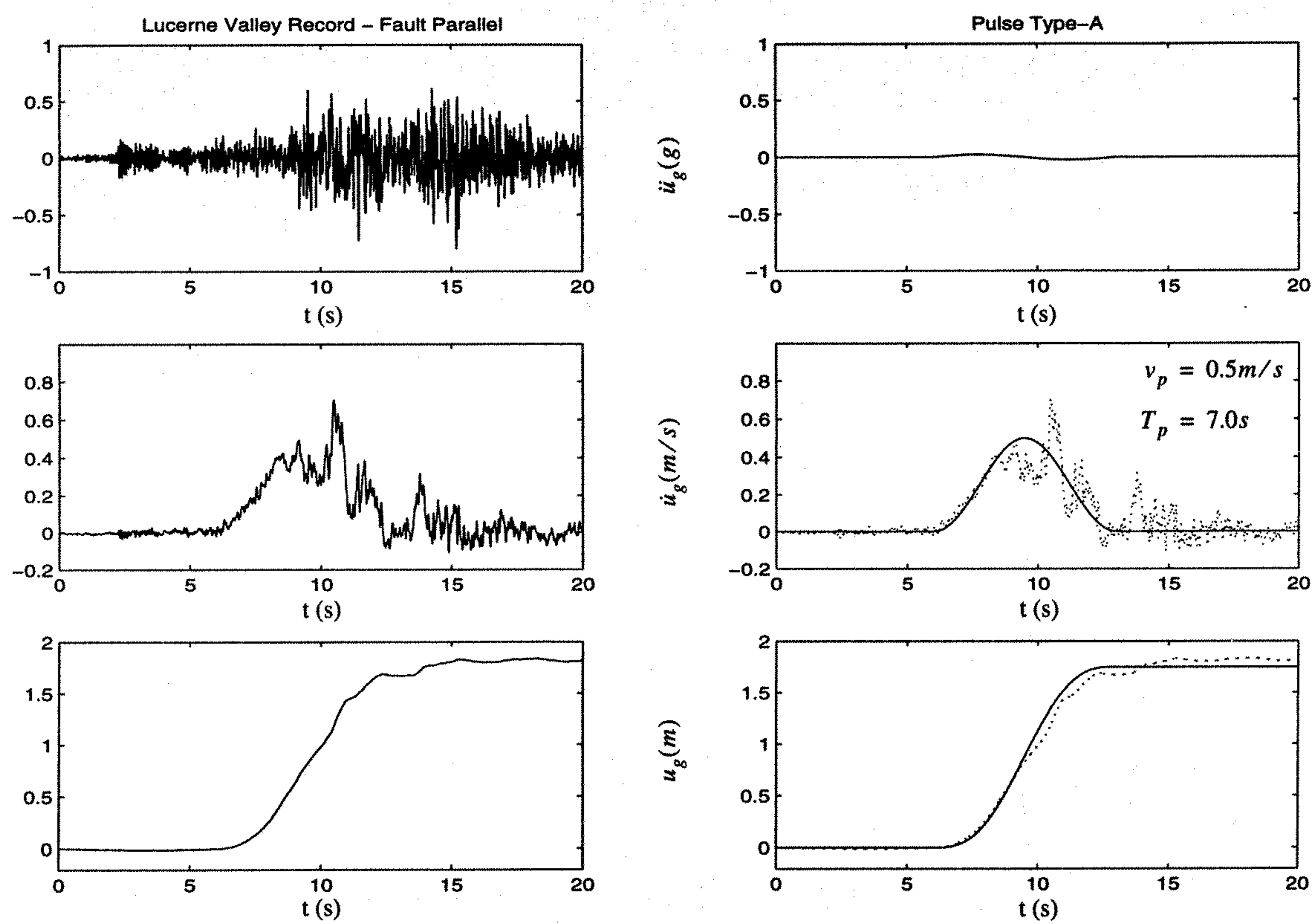

Figure 6: Fault parallel components of the acceleration, velocity, and displacement time histories recorded at the Lucerne Valley station during the June 28th, 1992 Landers, California earthquake (left), and a cycloidal type-A pulse (right).

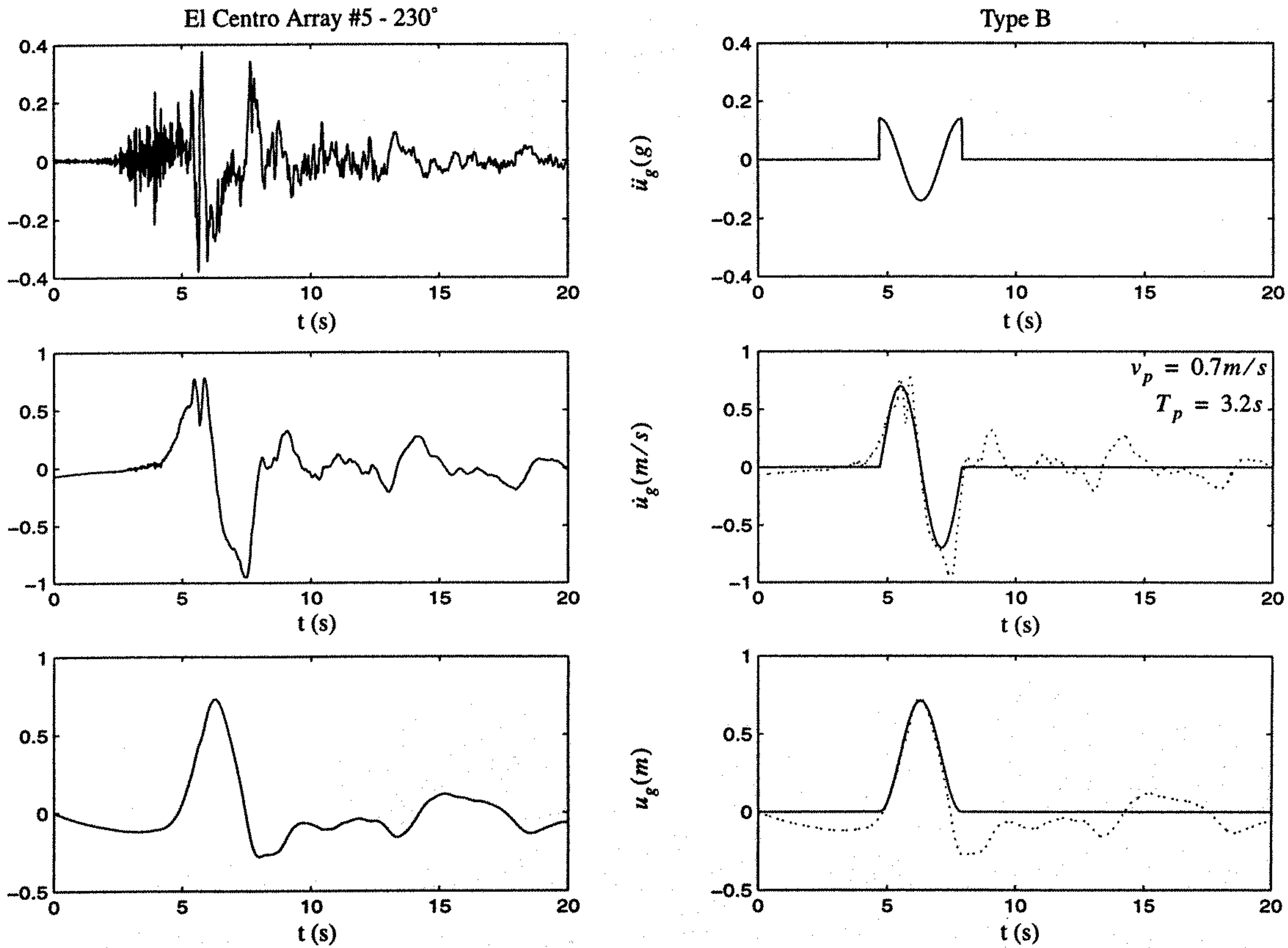

Figure 7: Fault normal components of the acceleration, velocity, and displacement time histories rerorded at the El Centro Array #5 station during the October 15th, 1979 Imperial Valley, California earthquake (left), and a cycloidal type-B pulse (right).

Figure 8 (left) portrays the fault-normal components of the acceleration, velocity, and displacement histories of the January 17th, 1994 Northridge earthquake recorded at the Rinaldi station. This motion resulted in a forward ground displacement that recovered partially. The velocity history has a large positive pulse and a smaller negative pulse that is responsible for the partial recovery of the ground displacement. Had the negative velocity pulse generated the same area as the positive velocity pulse, the ground displacement would have fully recovered. Accordingly, the fault normal component of the Rinaldi station record is in between a forward and a forward-and-back pulse. Figure 8 (center) shows the results of equations (4.1) to (4.3) by assuming a pulse duration Tp=0.8 s and a velocity amplitude V_p=1.75 m/s which are approximations of the duration and velocity amplitude of the first main pulse shown in the record. Figure 8 (right) shows the results of equations (4.4) to (4.6) by considering a pulse duration T_p=1.3 s and a velocity amplitude V_p=1.3 m/s. A similar situation prevails for the fault normal motion recorded at the Lucerne Valley station during the June 18th, 1992 Landers earthquake, which is shown in Figure 9 (left). Again, the velocity history has a large negative pulse that is followed by a smaller positive pulse. Had the second positive pulse generated the same area as the negative pulse, the ground displacement would have fully recovered. Figure 9 (center) shows the results of equations (4.1) to (4.3) by considering a pulse duration T_p=3.0 sec. and a velocity amplitude V_p=1.0 m/s which are approximations of the duration and velocity amplitude of the first main pulse shown in the record. Figure 9 (right) shows the results of equations (4.4) to (4.6) by considering a pulse duration T_p=5.0 s and a velocity amplitude of V_p=1.0 m/s. Trends similar to those observed in Figure 6 are also present in Figure 9. Although the constructed displacement and velocity histories either with a type-A pulse or a type-B pulse are capturing distinct elements of the kinematics of the recorded motion, the resulting ground acceleration is an order of magnitude smaller than the peak recorded value.

Not all near-source records are forward or forward-and-back pulses. Figure 10 (left) portrays the fault-normal component of the acceleration, velocity, and displacement time histories recorded at the Sylmar station during the January 17th, 1994 Northridge earthquake. The ground displacement consists of two main long-period cycles, the first cycle being the largest, and the subsequent ones decaying. These long period pulses are also distinguishable in the ground velocity history whsere the amplitude of the positive pulses is larger than the amplitude of the negative pulses. Figure 11 (left) portrays the fault parallel components of the acceleration, velocity, and

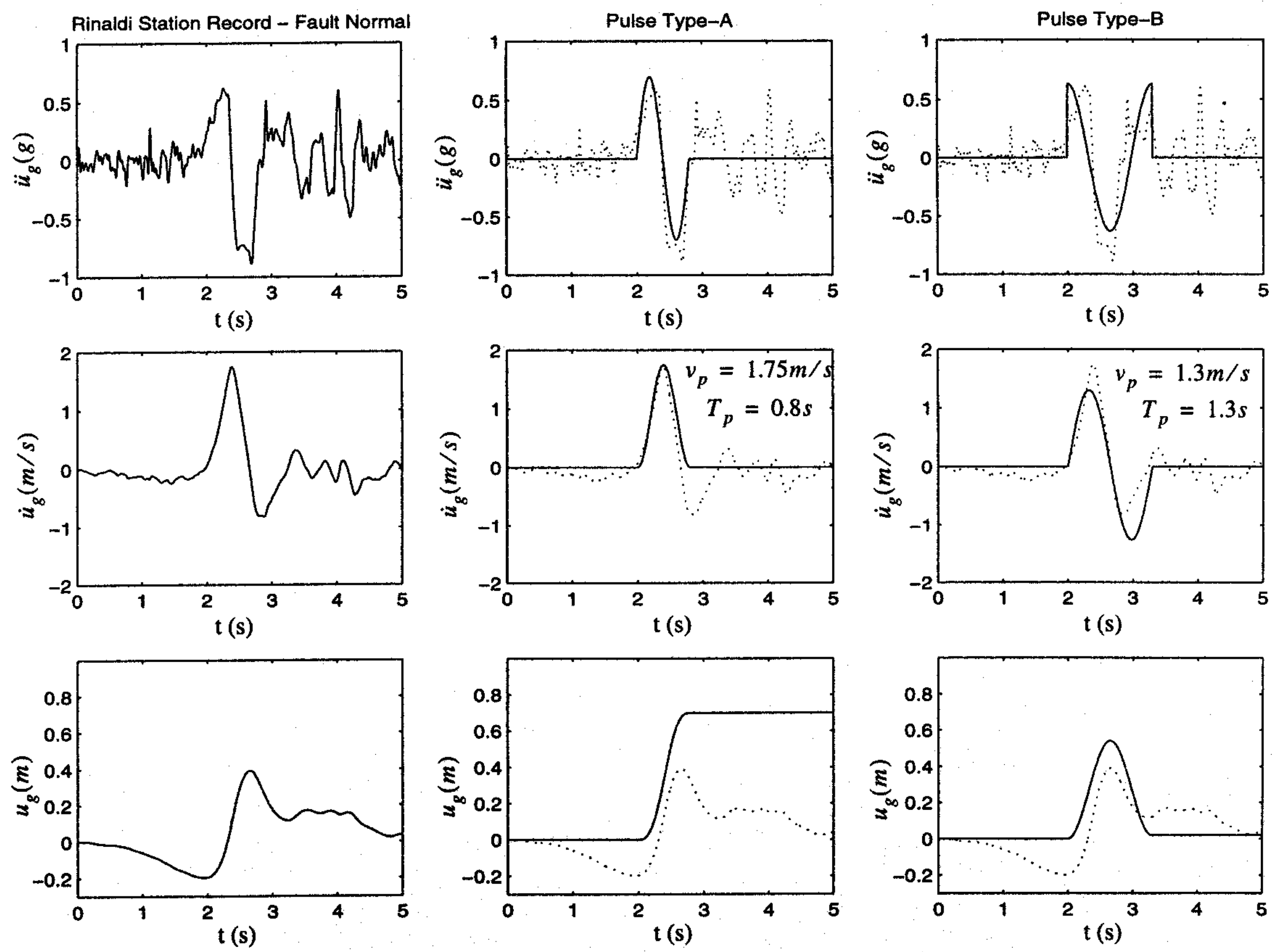

Figure 8: Fault normal components of the acceleration, velocity, and displacement time histories recorded at the Rinaldi station during the January 17th, 1994 Northridge, California earthquake (left), a cycloidal type-A pulse (center), and a cycloidal type-B pulse (right).

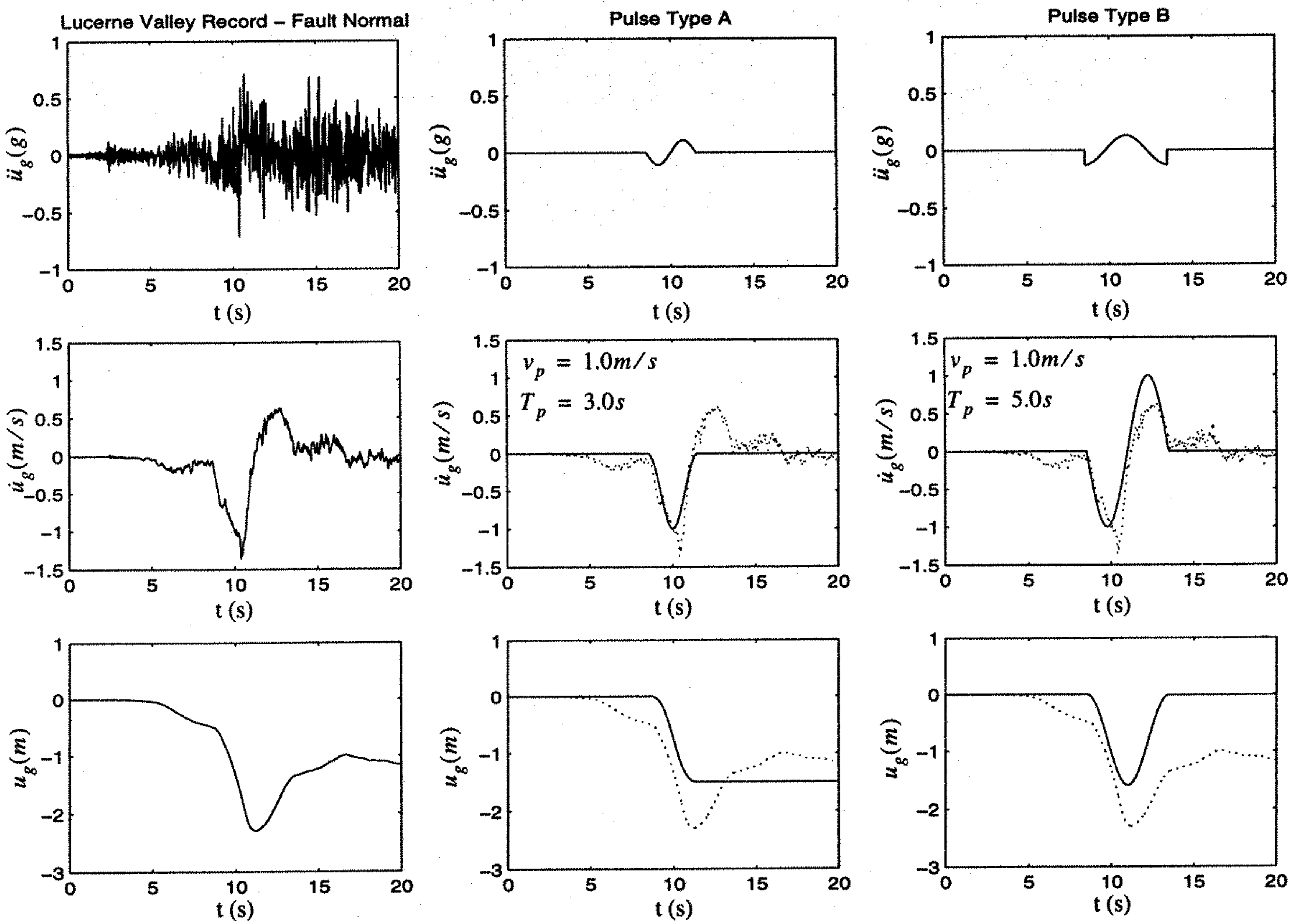

Figure 9: Fault normal components of the acceleration, velocity, and displacement time histories recorded at the Lucerne Valley station during the June 28th, 1992 Landers, California earthquake (left), a cycloidal type-A pulse (center), and a cycloidal type-B pulse (right).

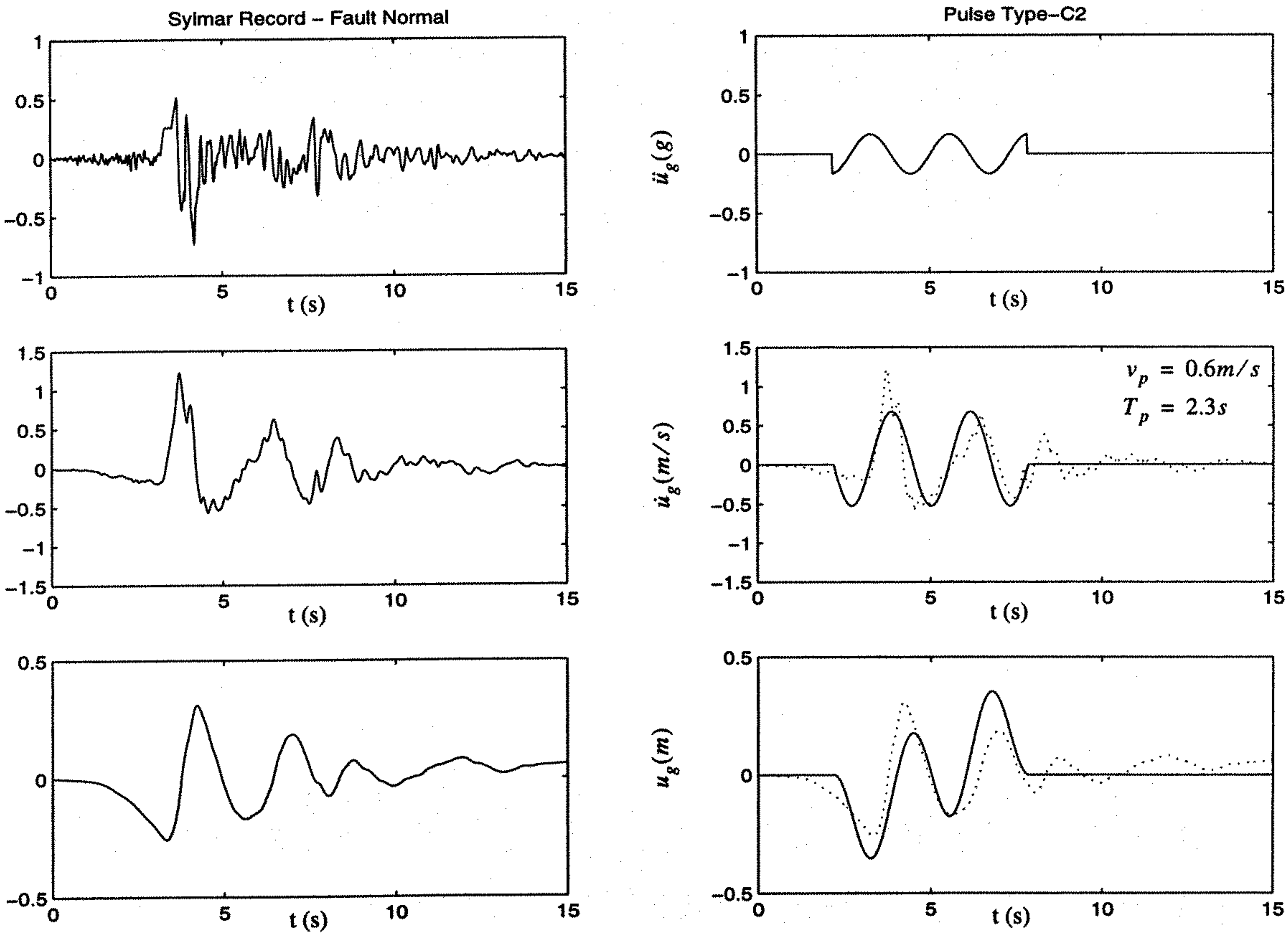

Figure 10: Fault normal components of the acceleration, velocity, and displacement time histories recorded at the Sylmar station during the January 17th, 1994 Northridge, California earthquake (left), and a cycloidal type-C_2 pulse (right).

displacement histories recorded at the Rinaldi station during the January 17th, 1994 Northridge earthquake. The ground displacement consists of two main long period cycles and subsequently the motion decays. These near-fault ground motions, where the displacement history exhibits one or more long duration cycles, are approximated with type-C pulses. A one-cycle ground displacement is approximated with a type-C_1 pulse that is defined as

$$\ddot{u}_g(t) = \omega_p v_p \sin(\omega_p t + \varphi), \quad 0 \le t \le \left(1.5 - \frac{\varphi}{\pi}\right)T_p \tag{4.7}$$

$$\dot{u}_g(t) = v_p \cos(\omega_p t + \varphi) - v_p \sin(\varphi), \quad 0 \le t \le \left(1.5 - \frac{\varphi}{\pi}\right)T_p \tag{4.8}$$

$$u_g(t) = -\frac{v_p}{\omega_p}\cos(\omega_p t + \varphi) - v_p t \sin(\varphi) + \frac{v_p}{\omega_p}\cos(\varphi), \quad 0 \le t \le \left(1.5 - \frac{\varphi}{\pi}\right)T_p \tag{4.9}$$

Figure 12 (third column) plots the acceleration, velocity, and displacement histories of a type-C_1 pulse given by equations (4.7) to (4.9). In deriving this expression it is required that the displacement and velocity are differentiable signals. The value of the phase angle, φ, is determined by requiring that the ground displacement at the end of the pulse is zero. A type-C_1 pulse with frequency $\omega_p = 2\pi/T_p$ has duration $T = 1.5T_p - 2\varphi/\omega_p = (1.5 - \varphi/\pi)T_p$. In order to have a zero ground displacement at the end of a type-C_1 pulse

$$\int_0^{(1.5 - \varphi/\pi)T_p} \dot{u}_g(t)dt = 0 \tag{4.10}$$

Equation (4.10), after evaluating the integral, gives

$$\cos(3\pi - \varphi) + (3\pi - \varphi)\sin\varphi - \cos\varphi = 0 \tag{4.11}$$

The solution of the transcendental equation given by (4.11) gives the value of the phase $\varphi = 0.0697\pi$ for a type-C_1 pulse.

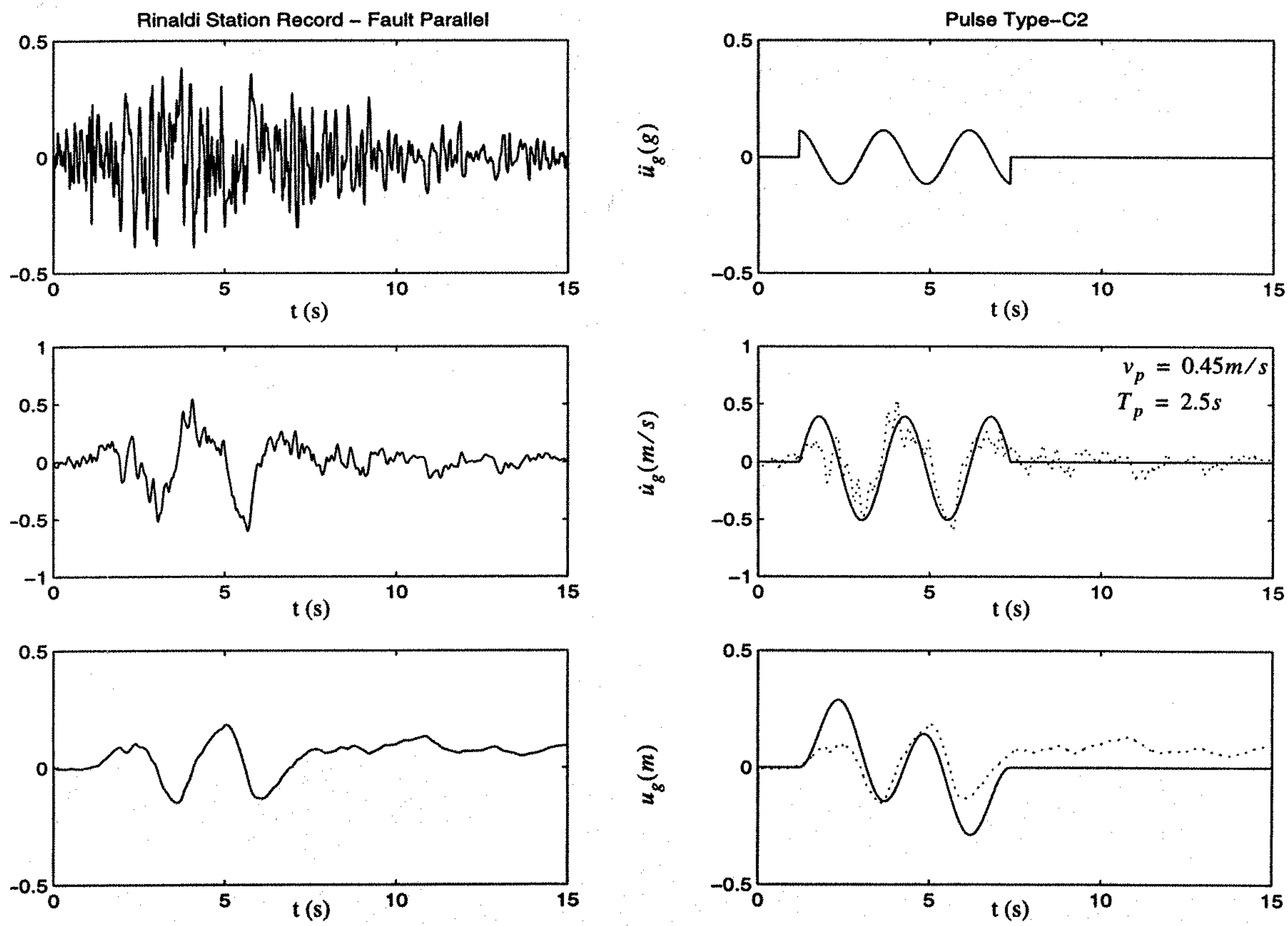

Figure 11: Fault parallel components of the acceleration, velocity, and displacement time histories recorded at the Rinaldi station during the January 17th, 1994 Northridge, California earthquake (left), and a cycloidal type-C_2 pulse (right).

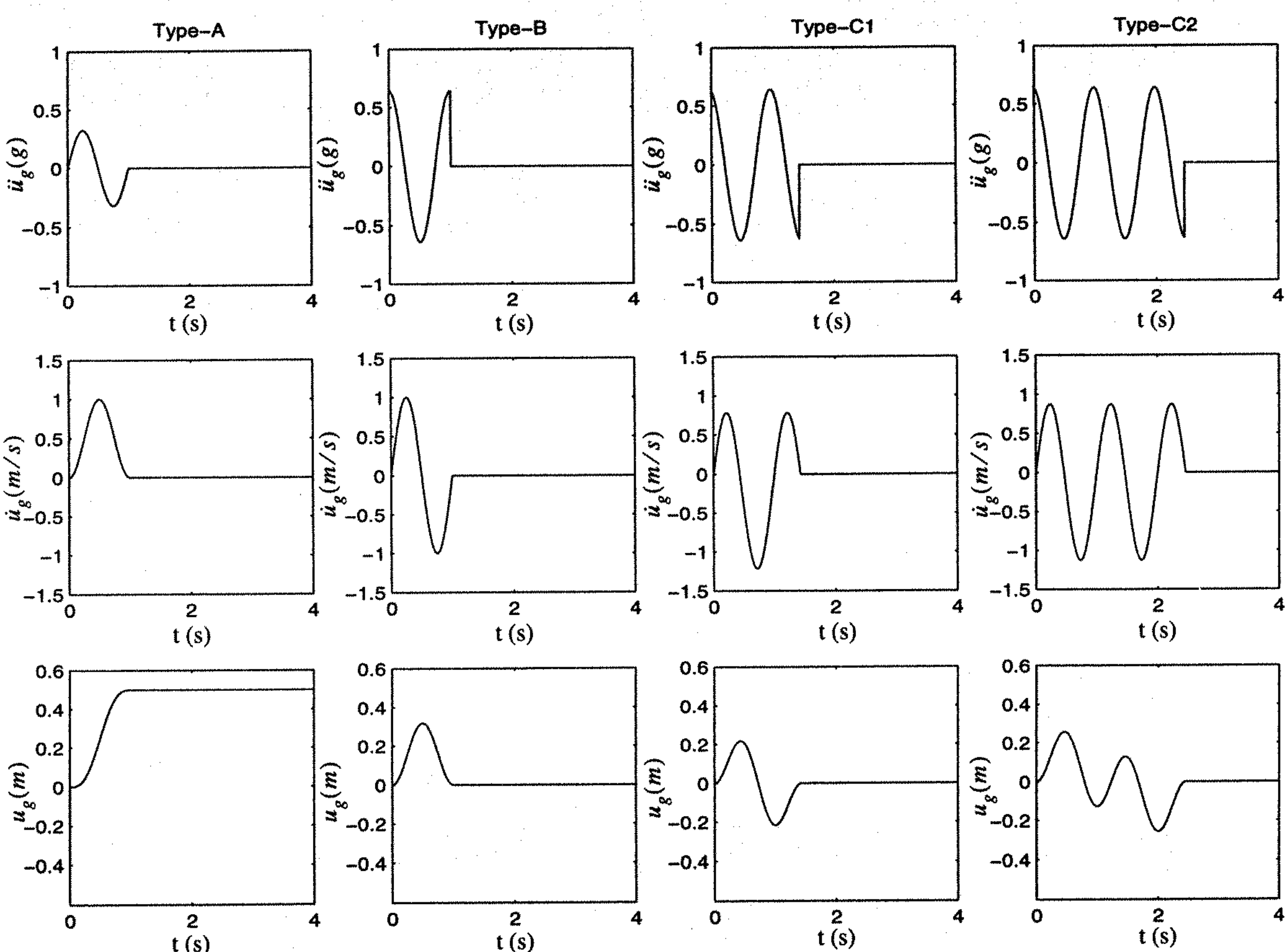

Figure 12: Acceleration, velocity, and displacement time histories of cycloidal pulses type-A (first column), type-B (second column), type-C1 (third column), and type-C2 (fourth column).

A two-cycle ground displacement is approximated with a type-C_2 pulse which is described by the same equations (4.7) to (4.9). A type-C_2 pulse has duration $T = 2.5T_p - 2\varphi/\omega_p = (2.5 - \varphi/\pi)T_p$. The condition for a zero ground displacement at the end of a type-C_2 pulse gives

$$\cos(5\pi - \varphi) + (5\pi - \varphi)\sin\varphi - \cos\varphi = 0 \tag{4.12}$$

The solution of (4.12) gives the value of $\varphi = 0.0410\pi$ for a type-C_2 pulse. Figures 11 and 12 (right) plot the acceleration, velocity, and displacement histories of a type-C_2 pulse.

A type-C_n pulse is expressed by

$$\ddot{u}_g(t) = \omega_p v_p \sin(\omega_p t + \varphi)\ ,\ \ 0 \le t \le \left(n + \frac{1}{2} - \frac{\varphi}{\pi}\right)T_p \tag{4.13}$$

$$\dot{u}_g(t) = v_p \cos(\omega_p t + \varphi) - v_p \sin(\varphi)\ ,\ \ 0 \le t \le \left(n + \frac{1}{2} - \frac{\varphi}{\pi}\right)T_p \tag{4.14}$$

$$u_g(t) = -\frac{v_p}{\omega_p}\cos(\omega_p t + \varphi) - v_p t \sin(\varphi) + \frac{v_p}{\omega_p}\cos(\varphi)\ ,\ \ 0 \le t \le \left(n + \frac{1}{2} - \frac{\varphi}{\pi}\right)T_p \tag{4.15}$$

where the phase, φ, is the solution to the transcendental equation

$$\cos[(2n+1)\pi - \varphi] + [(2n+1)\pi - 2\varphi]\sin\varphi - \cos\varphi = 0 \tag{4.16}$$

As n increases, a type-C_n pulse tends to a harmonic steady-state excitation. Figure 12 summarizes the acceleration, velocity, and displacement shapes of a forward-pulse, a forward-and-back pulse, a type-C_1, and a type-C_2 pulse. The displacement of a forward-and-back pulse has the same shape as the velocity of a forward pulse. Similarly, the shape of the displacement of a type-C_1 pulse resembles the shape of the velocity of a forward-and-back pulse and the shape of the acceleration of a forward pulse. This shows that type-C pulses provide a continuous transition from cycloidal pulses to harmonic steady-state motions.

CHAPTER 5
RESPONSE TO A ONE-SINE PULSE (TYPE-A PULSE)

Chapter 4 indicates that the kinematic characteristics of certain ground motions that result in a considerable permanent ground displacement can be described with a one-sine pulse also known as a cycloidal pulse of type A. The linear rocking response of a rigid block subjected to a one-sine pulse can be computed with (2.10), (2.11), (2.15), and (2.16). Figure 13 plots the response of the rigid block (b=0.2m and h=0.6 m) subjected to a one-sine pulse excitation with duration of 1sec ($\omega_p = 2\pi$). The solid line is the analytical solution presented in Chapter 2, and the dashed line is the result of the linear formulation of the numerical solution presented in Chapter 8. The agreement between the two solutions validates the performance of the numerical algorithm. On the left of Figure 13, the amplitude of the acceleration pulse is $a_p = 3.825\ \text{m/sec}^2$ (0.3899g) and the block does not overturn, whereas on the right of Figure 13, $a_p = 3.826\ \text{m/sec}^2$ (0.3900g) and the block overturns. Figure 13 indicates that, under a one-sine input, the block also overturns during free vibration. However, the acceleration amplitude needed to overturn the block during a one-sine pulse is less than the acceleration amplitude required to overturn the block during a half-sine pulse (compare the results of Figure 13 with Figure 2). Another important difference between the responses shown in Figures 2 and 14 is that, under a half-sine pulse, the block overturns at the end of the first quarter cycle, whereas under a one-sine pulse, the block overturns at the end of the third quarter cycle after experiencing one impact. This reversal of the angle of rotation before overturning does not allow for the derivation of a closed form expression that will yield the minimum acceleration needed to overturn the block. It becomes clear, however, that, under a type-A pulse, the value of the coefficient of restitution affects the value of the critical overturning acceleration, since the block experiences one impact before overturning. Consequently, even the linear solution for the minimum overturning accelerations is angle dependent since the coefficient of restitution, r, is a function of the slenderness of the block, α. The results presented herein are for the maximum value of the coefficient of restitution given by (2.6).

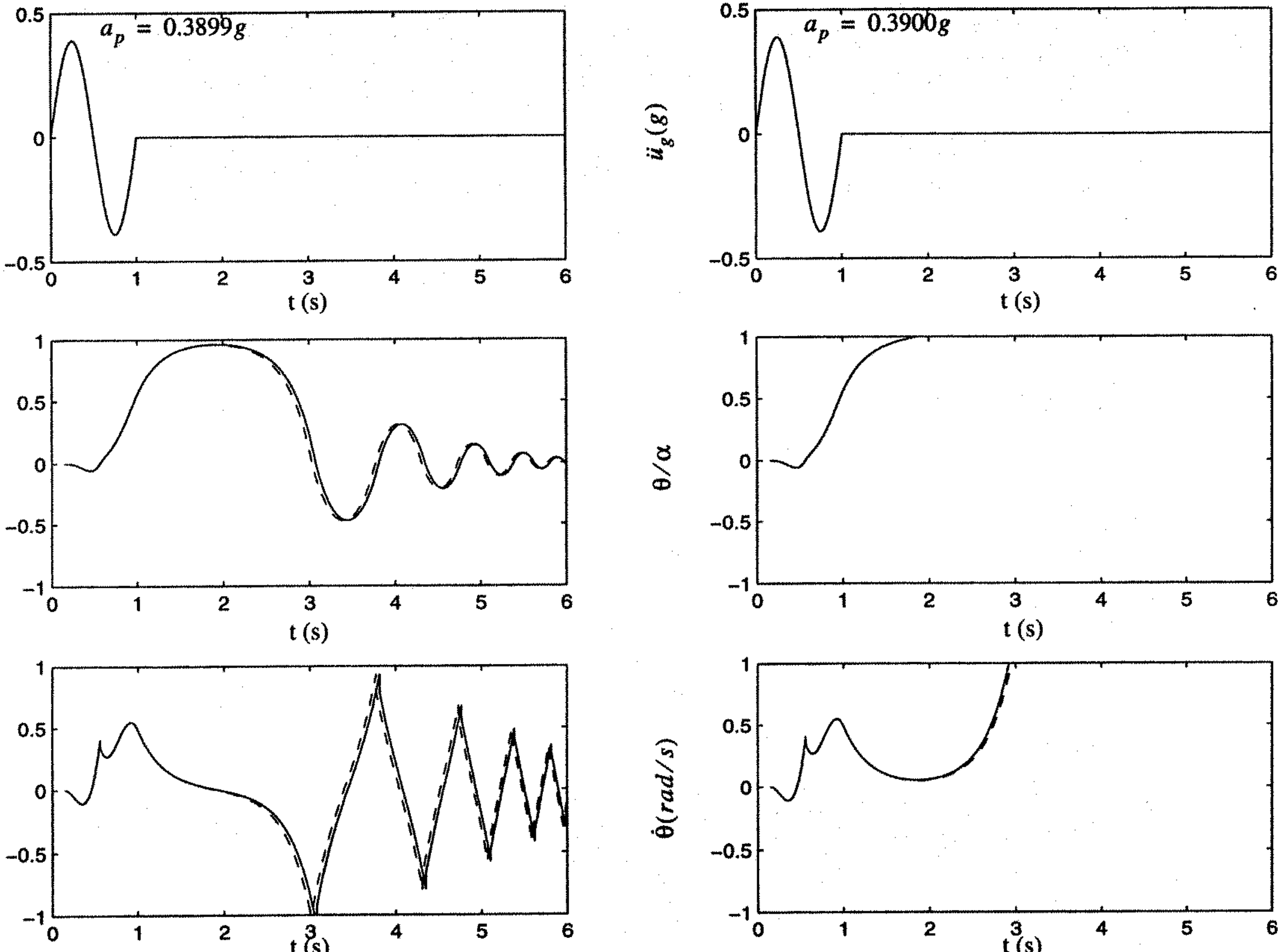

Figure 13: Rotation and angular velocity time histories of a rigid block (b=0.2 m, h=0.6 m) subjected to a one-sine pulse excitation. Left: no overturning. Right: overturning. Solid lines: analytical solution. Dashed: numerical solution with linear formulation.

Figure 14 presents the same study for a larger but geometrically similar block (b=0.5 m and h=1.5 m) subjected to the full-sine pulse excitation with $\omega_p = 2\pi$. On the left of Figure14, the amplitude of the acceleration pulse is a_p=4.426 m/sec^2 (0.4513g) and the block does not overturn, whereas on the right of Figure 14, a_p=4.429 m/sec^2 (0.4514g) and the block overturns. Again, overturning occurs during free vibration, during the third quarter cycle, after the block has experienced one impact.

The minimum acceleration amplitude of a one-sine pulse needed to overturn a rigid block with slenderness α is plotted on Figure 15 (top). Results are computed for $\alpha = 10°$, $20°$, and $30°$ with the nonlinear formulation that is presented in Chapter 8 and are compared with the linear solution for the minimum overturning acceleration of a half-sine excitation (equation (3.8)). It is shown that, for a one-sine pulse (type-A pulse), a considerably smaller acceleration amplitude is needed to overturn a block, since in this case the ground decelerates during the second half of the pulse. It is observed that the solution for $\alpha = 30°$ exhibits a stiffening effect for $\omega_p/p > 2.5$, while for $\alpha \le 20°$, Figure 15 (top) indicates that the minimum overturning acceleration amplitude, a_{po}, is a nearly linear function of ω_p/p in the frequency range of interest $(\omega_p/p < 3.0)$, which can be approximated with

$$\frac{a_{po}}{\alpha g} \approx 1 + \frac{1}{6}\frac{\omega_p}{p} \tag{5.1}$$

From equation (4.1), the velocity amplitude of the one-sine pulse is $v_p = 2a_p/\omega_p$, and for a slender rectangular block, the minimum overturning velocity amplitude, v_{po}, of a one-sine pulse can be approximated with

$$v_{po} = \frac{a_{po}T_p}{\pi} \approx 2\alpha\left(\frac{T_p g}{2\pi} + \frac{1}{3}\sqrt{\frac{Rg}{3}}\right) \tag{5.2}$$

The results of the approximate expression given by (5.2) are shown in Figure 15 (bottom) next to the results derived from the nonlinear numerical solution. The multiplication factor 1/3 of the size term in equation (5.2) indicates that the size of the block, R, has a weaker effect in preventing top-

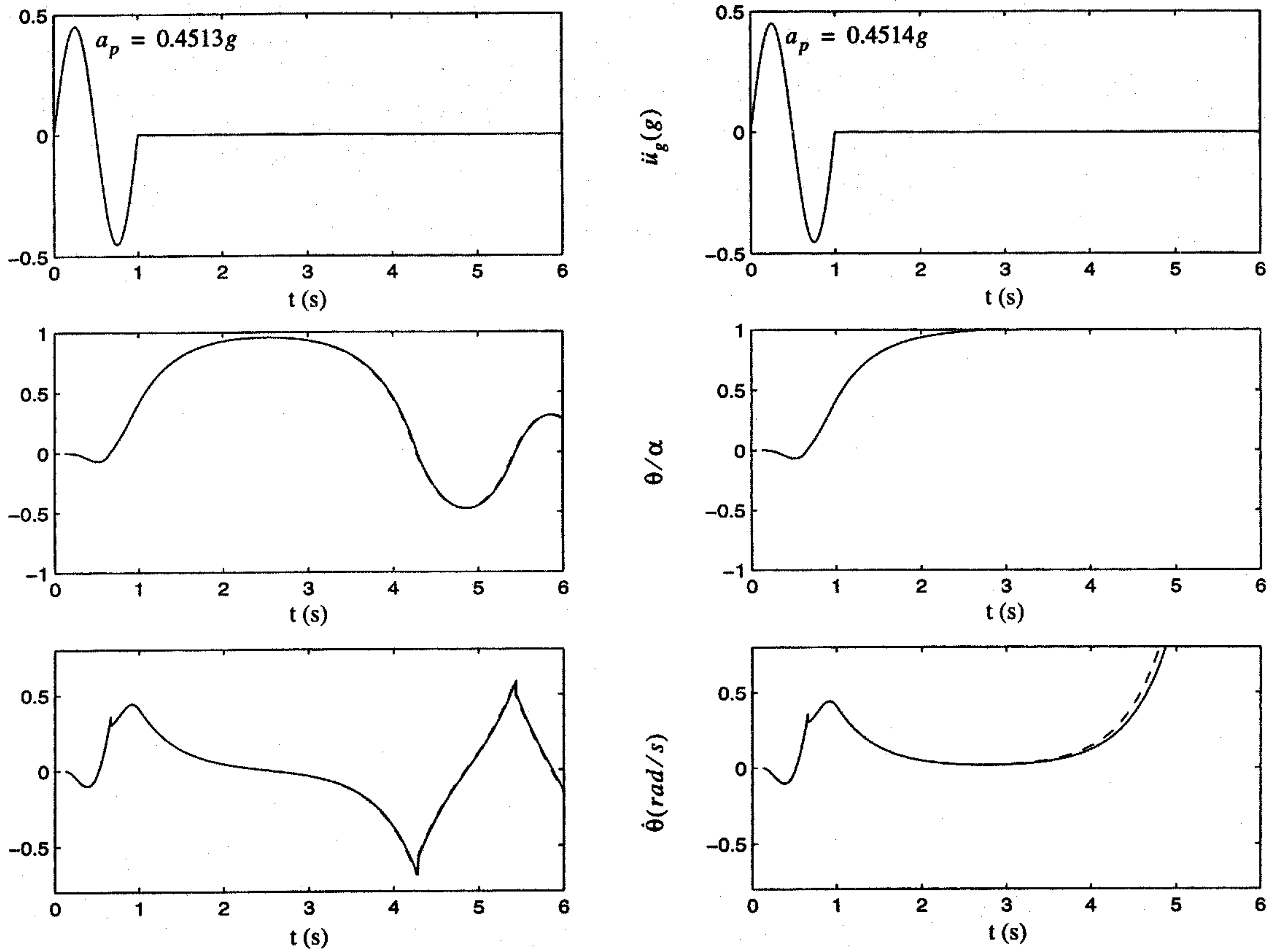

Figure 14: Rotation and angular velocity time histories of a rigid block (b=0.5 m, h=1.5 m) subjected to a one-sine pulse excitation. Left: no overturning. Right: overturning. Solid lines: analytical solution. Dashed: numerical solution with linear formulation.

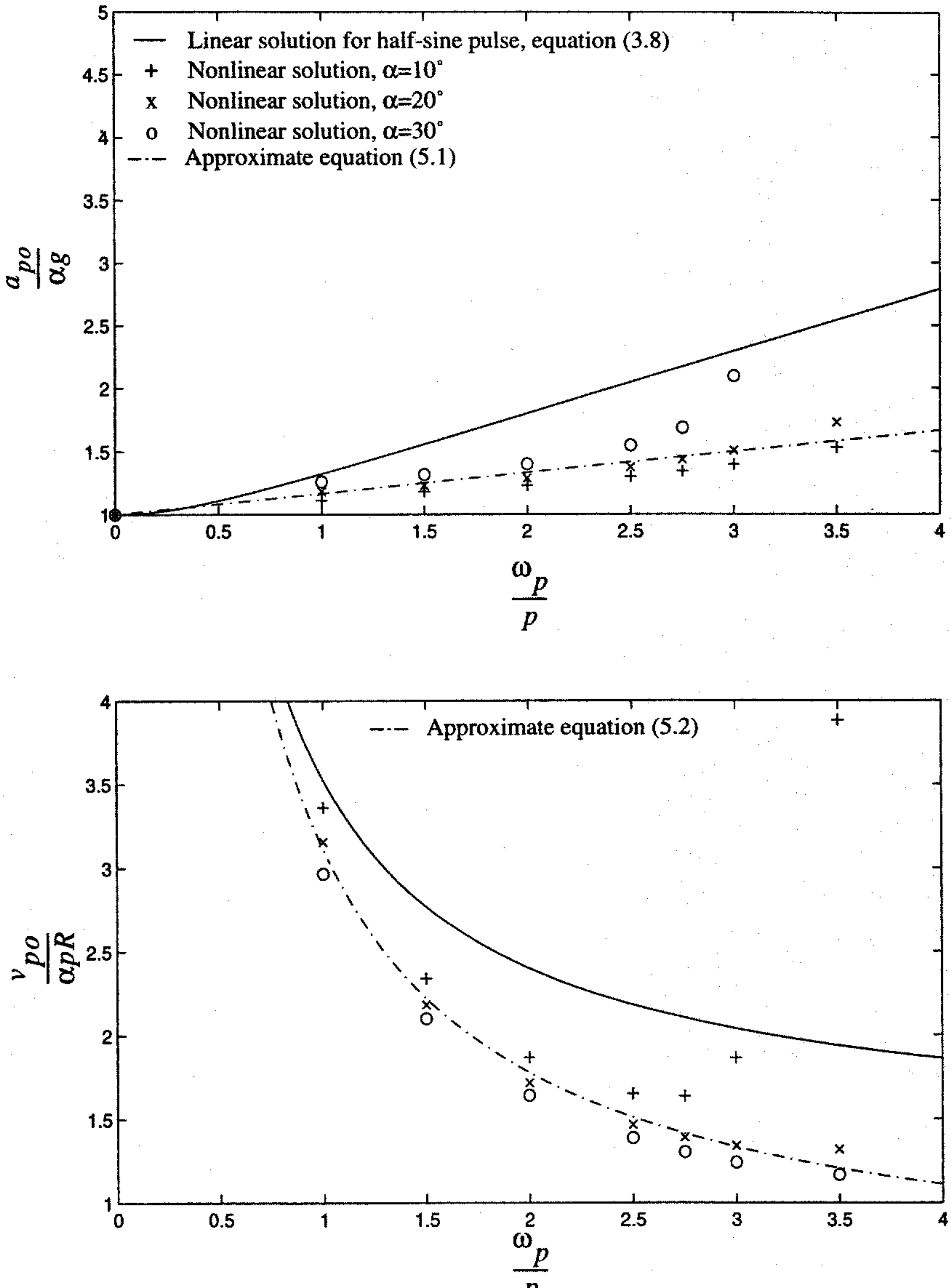

Figure 15: Spectrum of the minimum acceleration amplitude (top) and velocity amplitude (bottom) of a one-sine type-A pulse needed to overturn a free standing block.

pling than in the case of a half-sine pulse. As an example, consider the smaller block (b=0.2 m, h=0.6 m, R=0.632 m and ω_p/p =1.84) that is under investigation. Under a half-sine pulse with T_p=1 s, equation (3.10) indicates that whether the block overturns depends 48% on its size and 52% on the duration of the pulse. Under a one-sine pulse with T_p=1 s, equation (5.2) indicates that whether the block overturns depends 23.5% on its size and 76.5% on the pulse duration. Equation (5.2) indicates that the overturning of wide large blocks ($\alpha \geq 20°$ and $\omega_p/p \geq 2$) has a weaker dependence on the duration of the pulse than is the case with small and slender blocks.

CHAPTER 6

RESPONSE TO A ONE-COSINE PULSE (TYPE-B PULSE)

While some near source ground motions result in a forward pulse (non reversing pulse), other near-source ground motions result in a forward-and-back pulse where the ground dislocation recovers either fully or partially. The fault normal component of the El Centro Array #5 motion recorded during the October 15th, 1979 Imperial Valley earthquake and the Lucerne Valley motion recorded during the June 28th, 1992 Landers earthquake are examples of such forward-and-back pulses. In Chapter 4 it was shown that many of the features of these forward-and-back pulses can be captured with a one-cosine pulse (Pulse type-B). Figure 16 plots the response of the rigid block (b=0.5m and h=1.5m) subjected to a one-cosine pulse excitation with duration of 1 sec and $\omega_p = 2\pi$. On the left of Figure 16 the amplitude of the acceleration pulse is $a_p = 0.6245g$ and the block does not overturn, whereas on the right of Figure 16, $a_p = 0.6255g$ and the block overturns. Figure 16 indicates that, under a one-cosine pulse, the block again overturns during the free vibrations. However, now the acceleration amplitude needed to overturn the block with $\omega_p/p = 2.91$ is larger than the acceleration amplitude needed to overturn the same block during a one-sine pulse. The minimum acceleration amplitudes, a_{po}, of a one-cosine pulse needed to overturn a rigid block with slenderness α are plotted in Figure 17 (top). Results are computed for $\alpha = 10°$, $20°$, and $30°$ with the nonlinear formulation that is presented in Chapter 8.

Figure 17 (top) also indicates that the minimum overturning acceleration amplitude of a one-cosine pulse needed to overturn a block with an average slenderness of $\alpha = 20°$ can be approximated with the linear expression

$$\frac{a_{po}}{\alpha g} \approx 1 + \frac{1}{4}\frac{\omega_p}{p}. \qquad (6.1)$$

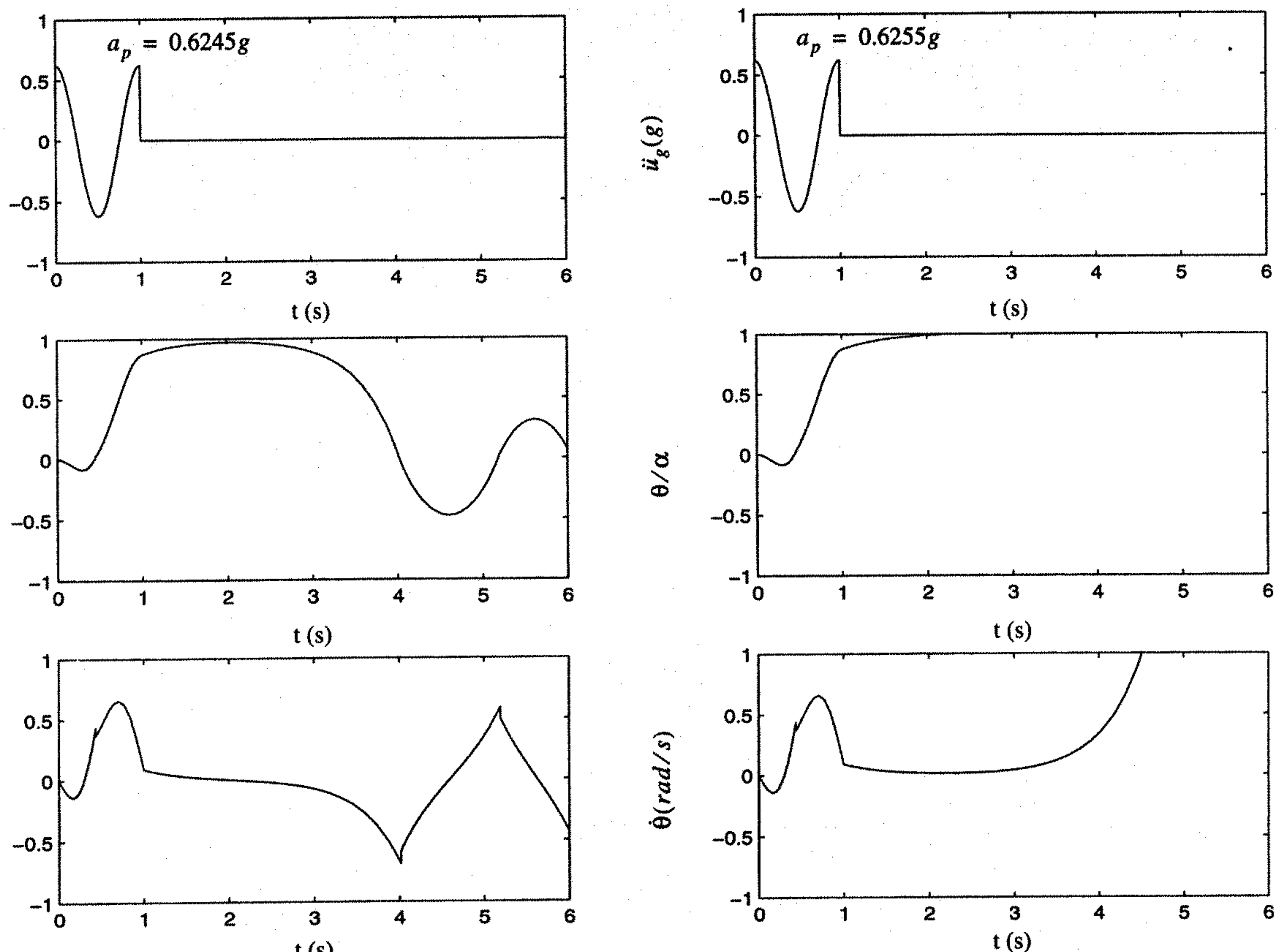

Figure 16: Rotation and angular velocity time histories of a rigid block (b=0.5 m, h=1.5 m) subjected to a type-B pulse excitation. Left: no overturning. Right: overturning.

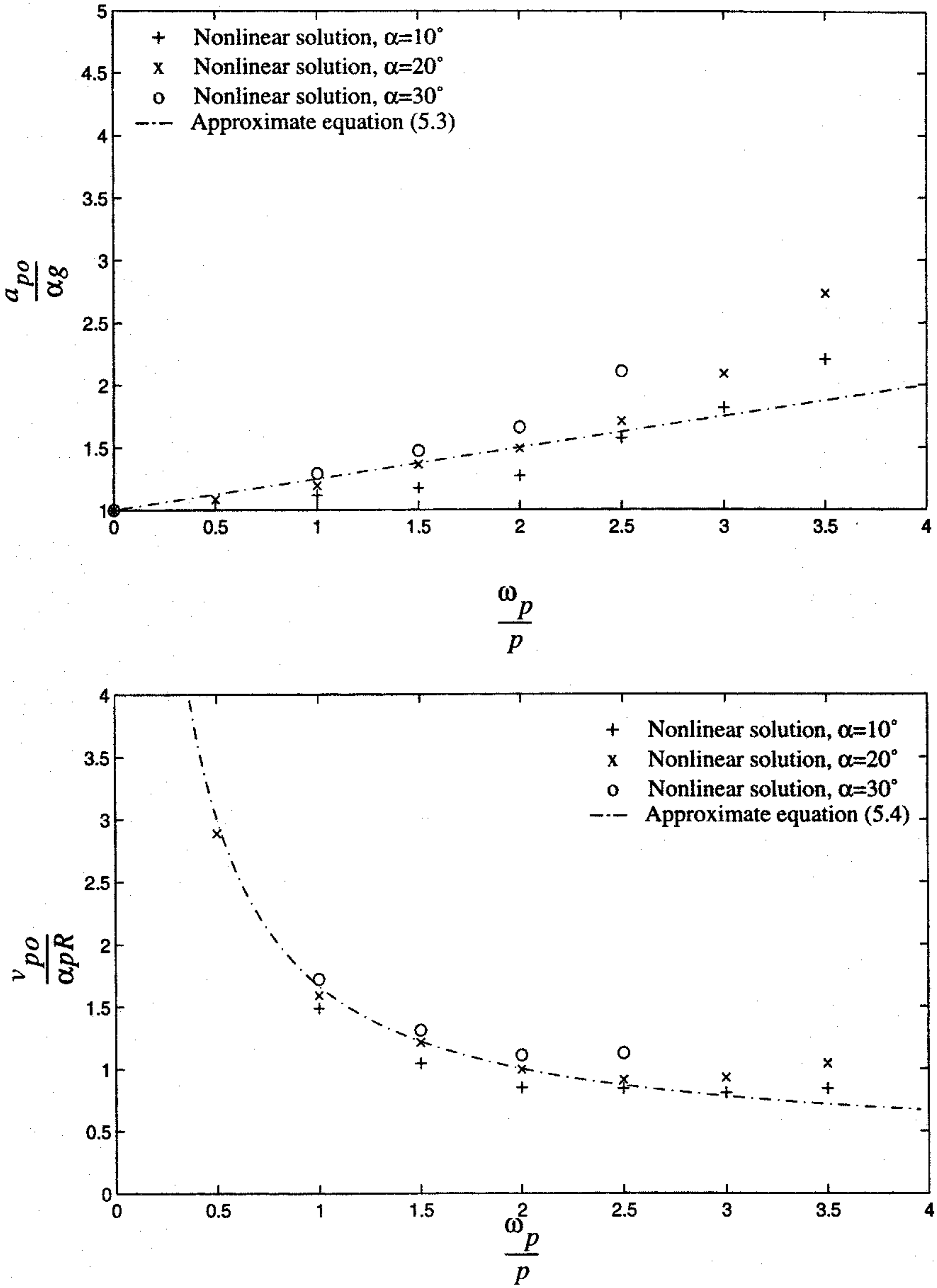

Figure 17: Spectrum of the minimum acceleration amplitude (top) and velocity amplitude (bottom) of a type-B pulse needed to overturn a free standing block.

From equation (4.4) the velocity amplitude of the one-cosine pulse is $v_p = a_p / \omega_p$, and, for a rectangular block, equation (6.1) gives

$$v_{po} = \frac{a_{po} T_p}{\pi} \approx \alpha\left(\frac{T_p g}{2\pi} + \frac{1}{2}\sqrt{\frac{Rg}{3}}\right). \tag{6.2}$$

The results of the approximate expression given by (6.2) are shown in Figure 17 (bottom) next to the results derived from the nonlinear numerical solution. The multiplication factor of the size term in (6.2) is 1/2, which indicates that for a one-cosine pulse the size, R, of a block has a weaker effect in preventing toppling than in the case of a half-sine pulse.

CHAPTER 7
RESPONSE TO TYPE-C PULSES

Figure 18 plots the response of the rigid block (b=0.2 m, h=0.6 m, p=3.41 rad/sec) subjected to the type-C_1 pulse given by equations (4.7) to (4.9) with T_p=1.0 sec $(\omega_p = 2\pi)$. On the left of Figure 18, the amplitude of the pulse is $a_p = 3.96 m/s^2$ (0.4037g) and the block does not overturn, whereas on the right of Figure 18, $a_p = 3.97 m/s^2$ (0.4047g) and the block overturns. In this case the block experiences an early rocking motion with small amplitudes that is followed by a large rotation. Figure 19 plots the response of the same block (b=0.2 m, h=0.6 m, p=3.41 rad/sec) subjected to a type-C_2 pulse with T_p=1.0 sec $(\omega_p = 2\pi)$. On the left of Figure 19 the amplitude of the pulse is $a_p = 3.89 m/s^2$ (0.3965 g) and the block does not overturn, whereas on the right of Figure 19, $a_p = 3.90 m/s^2$ (0.3976 g), and the block overturns. While there are many differences in the rocking motion of the block when subjected to a type-C_1 pulse and a type-C_2 pulse, the values of the overturning acceleration amplitudes for this case $(\omega_p/p = 1.84)$ are close.

The minimum acceleration amplitudes of a type-C_1 and a type-C_2 pulse needed to overturn a block with slenderness $\alpha = 20°$ are plotted on Figure 20 (top). For values of $\omega_p/p > 2.0$, the acceleration values increase with frequency at a larger rate. However, for values of $\omega_p/p \le 2.0$, Figure 20 (top) indicates that the minimum overturning acceleration amplitudes for both a type-C_1 and a type-C_2 pulse is a nearly linear function of ω_p/p, which can be approximated with

$$\frac{a_{po}}{\alpha g} \approx 1 + \frac{1}{6}\frac{\omega_p}{p} \tag{7.1}$$

The relation given by (7.1) is the same as the relation given by (5.1), which was derived for a type-A pulse. For the type-C pulse equations, equations (4.12) and (4.13) give that the velocity amplitude $v_p = a_p/\omega_p$, which is half the velocity amplitude that one obtains from a type-A pulse with the same acceleration amplitude a_p. Accordingly, for a slender block , the minimum overturning velocity amplitude of either a type-C_1 or type-C_2 pulse can be approximated with

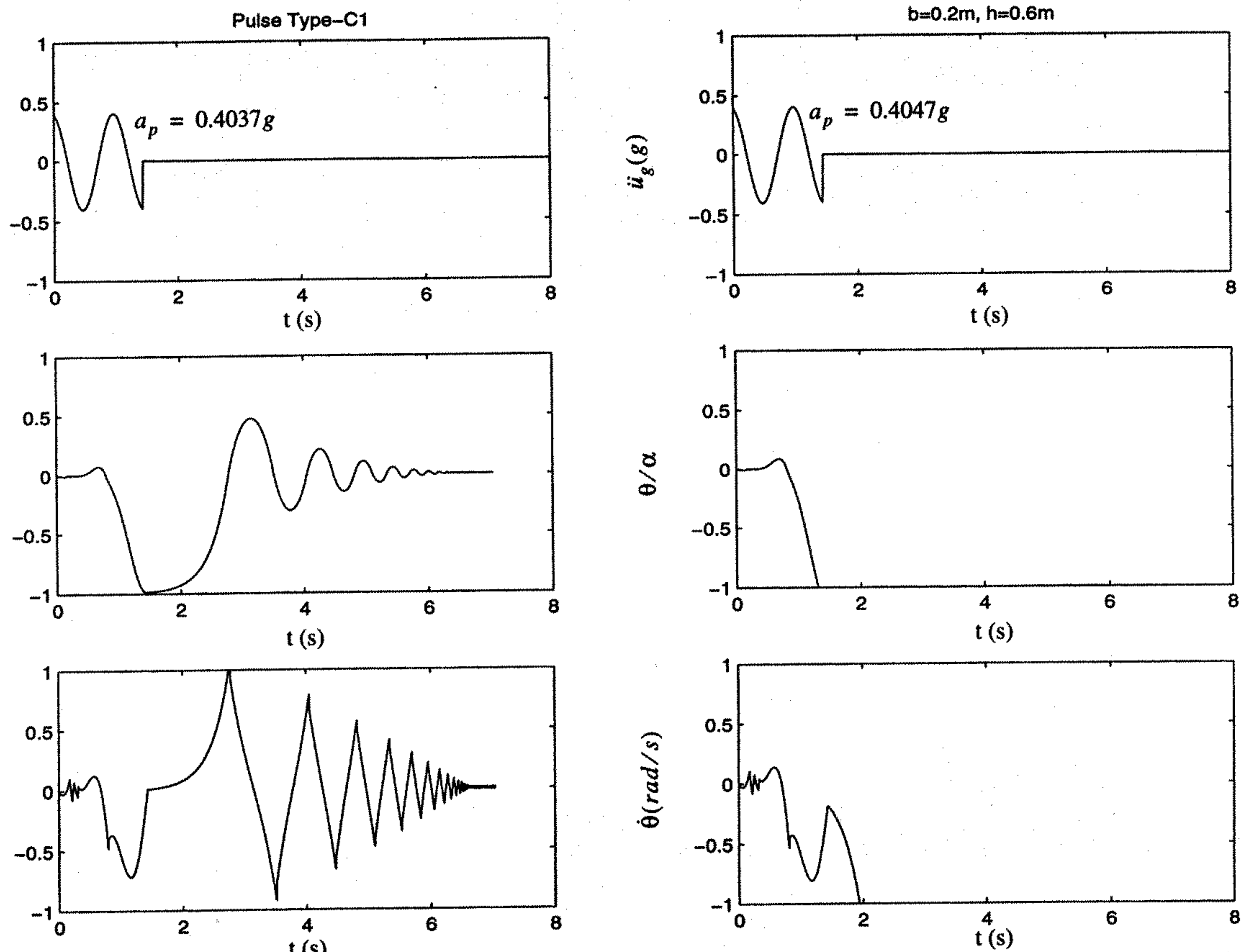

Figure 18: Rotation and angular velocity time histories of a rigid block (b=0.5 m, h=1.5 m) subjected to a type-C1 pulse excitation. Left: no overturning. Right: overturning.

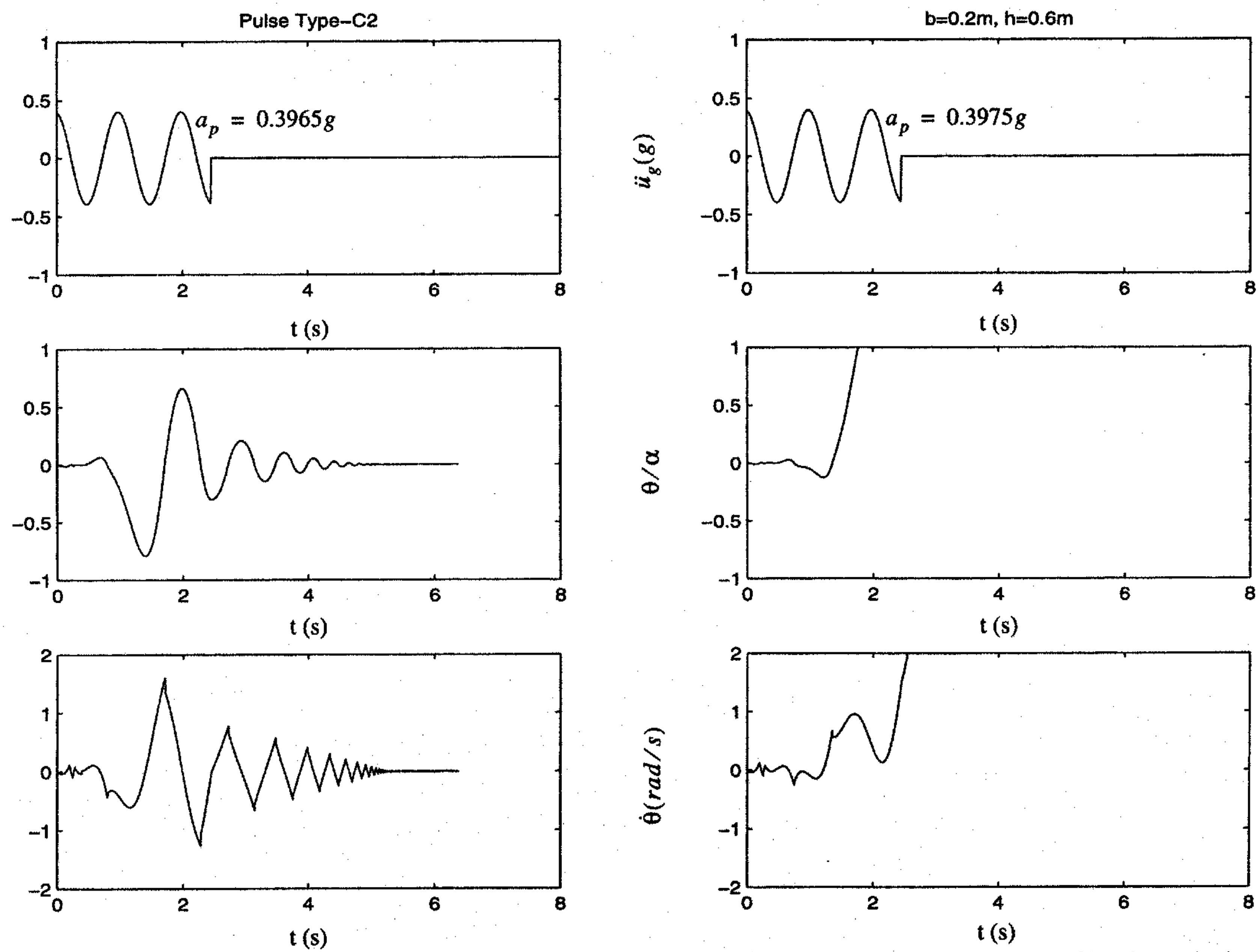

Figure 19: Rotation and angular velocity time histories of a rigid block (b=0.5 m, h=1.5 m) subjected to a type-C2 pulse excitation. Left: no overturning. Right: overturning.

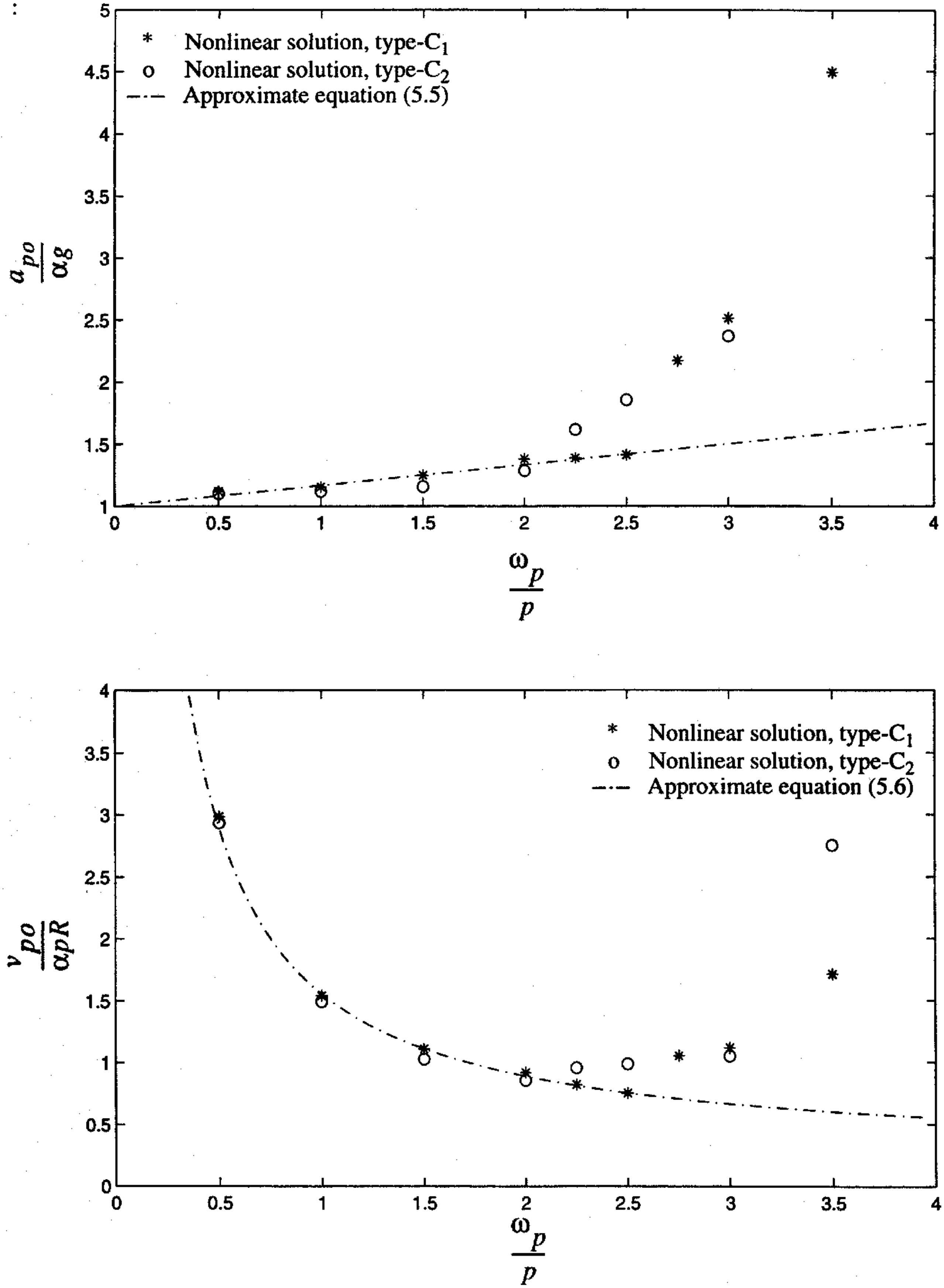

Figure 20: Spectra of the minimum acceleration amplitude (top) and velocity amplitude (bottom) of a type-C1 pulse (stars) and a type-C2 pulse (circles) required to overturn a free standing block.

$$v_p = \frac{a_p T_p}{\pi} = \alpha\left(\frac{T_p g}{2\pi} + \frac{1}{3}\sqrt{\frac{Rg}{3}}\right). \tag{7.2}$$

The results of the approximate expressions given by (7.2) are shown in Figure 20 (bottom) next to results obtained with the non-linear numerical solution for $\alpha = 20°$.

CHAPTER 8
NONLINEAR FORMULATION - NUMERICAL SOLUTION

The rocking response of a rigid block subjected to earthquake excitation is computed numerically via a state-space formulation which can accommodate the nonlinear nature of the problem. Similar integration of the equation of motion has been carried out by Yim et al. (1980), Spanos and Koh (1984), and Hogan (1989) among others. The state vector of the system is merely

$$\{y(t)\} = \begin{Bmatrix} \theta(t) \\ \dot{\theta}(t) \end{Bmatrix} \tag{8.1}$$

and the time-derivative vector f(t) is

$$f(t) = \{\dot{y}(t)\} = \begin{Bmatrix} \dot{\theta}(t) \\ (-p^2)\left[\sin(\alpha\,\mathrm{sgn}[\theta(t)] - \theta(t)) + \dfrac{\ddot{u}_g}{g}\cos(\alpha\,\mathrm{sgn}[\theta(t)] - \theta(t))\right] \end{Bmatrix} \tag{8.2}$$

For slender blocks, the linear approximation becomes dependable, and equation (8.2) reduces to

$$f(t) = \{\dot{y}(t)\} = \begin{Bmatrix} \dot{\theta}(t) \\ p^2\left[-\alpha\,\mathrm{sgn}[\theta(t)] + \theta(t) - \dfrac{\ddot{u}_g(t)}{g}\right] \end{Bmatrix} \tag{8.3}$$

The numerical integration of (8.2) or (8.3) is performed with standard ODE solvers available in MATLAB (1992). The fidelity of the numerical algorithm is validated in Figures 2, 14, and 15 where the numerical solution of the linear equations of motion given by (8.3) (dashed lines) is compared with the analytical solution given by (2.10), (2.11), and (2.15), (2.16) (solid lines). With the nonlinear formulation given by (8.2), the significance of the nonlinear nature of the problem is examined. The true minimum acceleration amplitudes of a half-sine pulse needed to overturn rigid blocks with various geometries are shown in Figure 4 and are compared with the correct linear solution given by (3.8) and the unconservative linear solution given by Housner (1963). The non-linear solution reveals that two blocks with the same size (same ω_p/p) will require different values of $a_p/(\alpha g)$ to be overturned. For instance, the normalized minimum acceleration needed to overturn a block with $\alpha=10^{o}$ is very close to the value obtained with the linear solution (equation (3.8)). However, when the slenderness of the block decreases ($\alpha=20^{o}$, $\alpha=30^{o}$) the normalized minimum acceleration needed to overturn the block increases. It so happens that these values lie in between the correct linear solution provided by equation (3.8) and the unconservative solution presented by Housner (1963). The nonlinear formulation was also used to compute the true minimum acceleration needed to overturn blocks with various slenderness when subjected to a cycloidal pulse type-A (Figure 15 (top)), a cycloidal pulse type-B (Figure 17 (top)), and cycloidal pulses type-C_n (Figure 20 (top)). Again, the value of the true normalized minimum acceleration required to overturn the block increases with α, showing that the linear solution is conservative. For these types of pulses, the solution for different values of the block angle, α, involves different values of the maximum coefficient of restitution r which depends on α through equation (2.6). It is interesting to note that, for $\alpha = 30°$, the true minimum acceleration needed to overturn a block has approximately two times the acceleration value resulting from the linear solution.

CHAPTER 9
RESPONSE TO SEISMIC EXCITATION

In Chapters 5, 6, and 7 we analyzed the rocking response of a free standing block subjected to three types of trigonometric pulses that can approximate some of the kinematic characteristics of near-source ground motions. We derived expressions to express the minimum overturning acceleration and velocity amplitudes of these pulses, and we concluded that, for small values of the frequency ratio $(\omega_p/p < 3)$, the toppling of a block depends on its slenderness, α, its size, R, and the duration of the pulse, T_p. In this chapter, the foregoing analysis is used to provide information on the stability of a block subjected to near-source ground motions.

The challenge with such motions is that, in many instances the main long duration pulse that generates the substantial displacements is jammed by high-frequency fluctuations that override along. For instance, this phenomenon is most apparent at the Caleta de Campos record, shown in Figure 5, and the Lucerne Valley records, shown in Figures 6 and 9. The El Centro Array #5 record, shown in Figure 7, contains few distinct fluctuations on top of the main pulse, whereas the Rinaldi station record, shown in Figure 8, is clear to the extend that the pulse motion is distinguishable even in the acceleration history.

Figure 8 indicates that the Rinaldi station record is in between a 0.8-second duration type-A pulse and a 1.3-sec duration type-B pulse. From equation (5.2), the minimum overturning velocity amplitude of a one-sine pulse with T_p=0.8 sec that is needed to overturn the 0.5m x 1.5m block ($\alpha = 18.45° = 0.3217$ rad, p=2.157 rad/s) is $v_{po} = 1.29$ m/s. Accordingly, since the velocity amplitude of the Rinaldi station record, when considered as a forward pulse, is approximately 1.75m/s, the approximation of the Rinaldi station motion with a one-sine pulse yields that 74% $(1.29/1.75 = 0.74)$ of the Rinaldi motion is sufficient to overturn the block. On the other hand, equation (6.2) indicates that the minimum overturning velocity amplitude of a one-cosine pulse with T_p = 1.3 sec that is needed to overturn the same block is $v_{po} = 1.02$ m/s. Now the approximation of the Rinaldi station to a one-cosine pulse yields that 78% $(1.02/1.30 = 0.78)$ of the Rinaldi motion is sufficient to overturn the block. Figure 21 (left) plots the rocking response of the 0.5m x 1.5m block subjected to the 75% level of the Rinaldi station motion at which the block

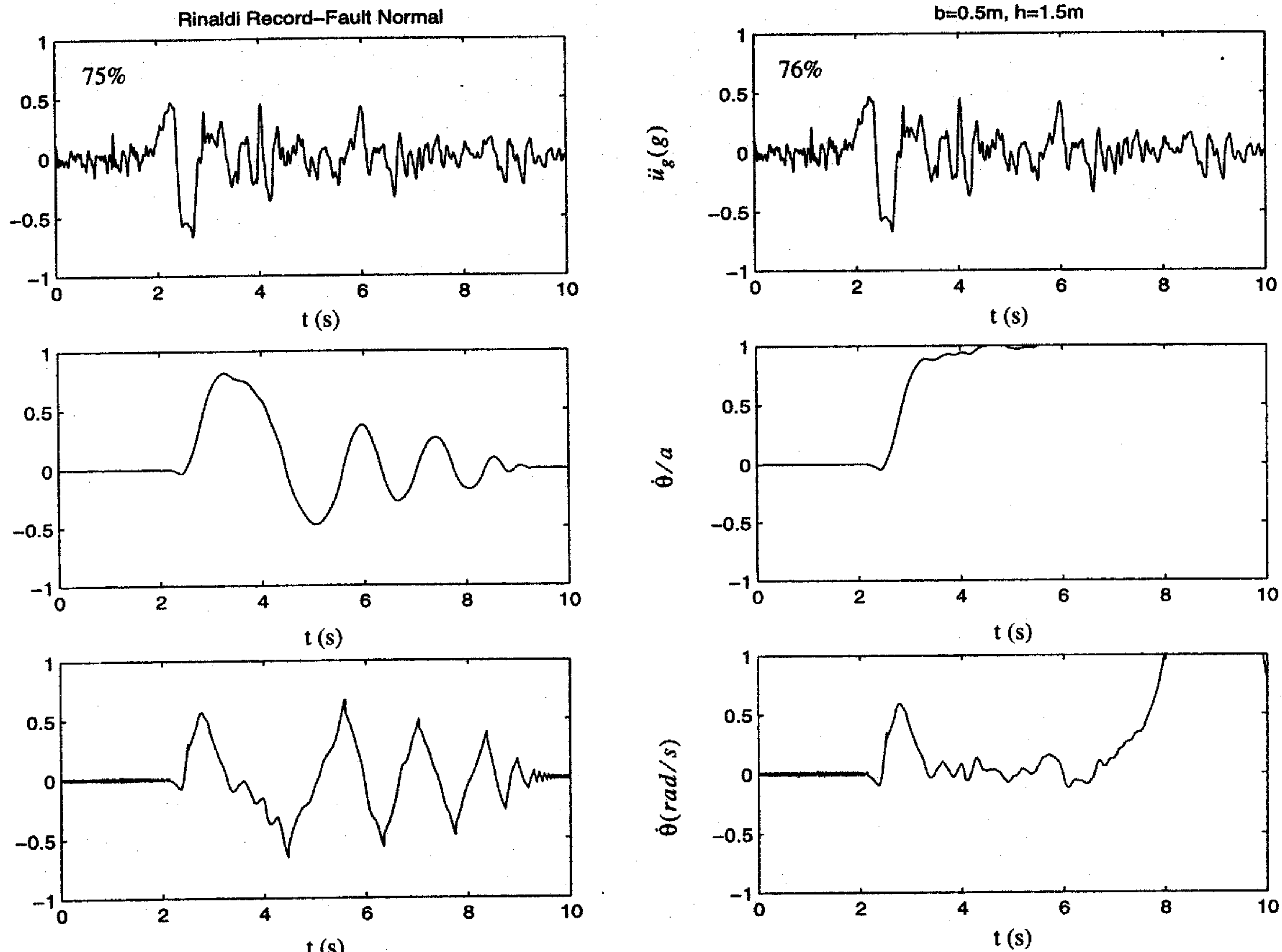

Figure 21: Rotation and angular velocity response time histories of a rigid block (b=0.5 m, h=1.5 m) subjected to the fault-normal Rinaldi station motion. Left: no overturning (75% acceleration level). Right: overturning (76% acceleration level).

does not overturn, whereas on the right of Figure 21, the block overturns when subjected to a 76% level of the Rinaldi station record. This level of 76% is between the levels of 74% and 78% that we computed with equations (5.2) and (6.2), respectively.

Figure 22 plots the minimum overturning velocity spectrum of the Rinaldi station motion by assuming a pulse frequency $\omega_p^A = 2\pi/0.8s = 2.5\pi$ rad/s. The velocity spectrum of a pulse type-A together with the solution of the approximate expression given by (5.2) are also shown in Figure 22. The good agreement of the results presented in Figure 22 indicates that the response values obtained from cycloidal pulses can provide dependable information on the overturning of a block when subjected to the Rinaldi station record.

Our analysis proceeds by investigating the rocking response of blocks to near source ground motions that contain a distinct long duration pulse as well as high frequency fluctuations that override along the long duration pulse. The question that arises with such records is whether a block will overturn due to the high frequency spike or due to the low acceleration, low frequency pulse.

This question is partially addressed by observing the forward-and-back motion recorded at the El Centro Array #5 station shown in Figure 7. At approximately 5.5 s, the velocity history displays a distinct fluctuation which is distinguishable in the acceleration history. Figure 23 plots the first 10 seconds of the El Centro Array #5 station record, and it can be observed that the local fluctuation BCDEFGH is nothing more than a type-C_1 pulse with approximate period $T_p^{C_1} \approx 0.4$ s and an approximate acceleration amplitude $a_p^{C_1} = \omega_p^{C_1} v_p^{C_1} = 0.27g$, which is twice the value of the acceleration amplitude $a_p^B = \omega_p^B v_p^B = 0.14g$ of the long duration pulse AIZ.

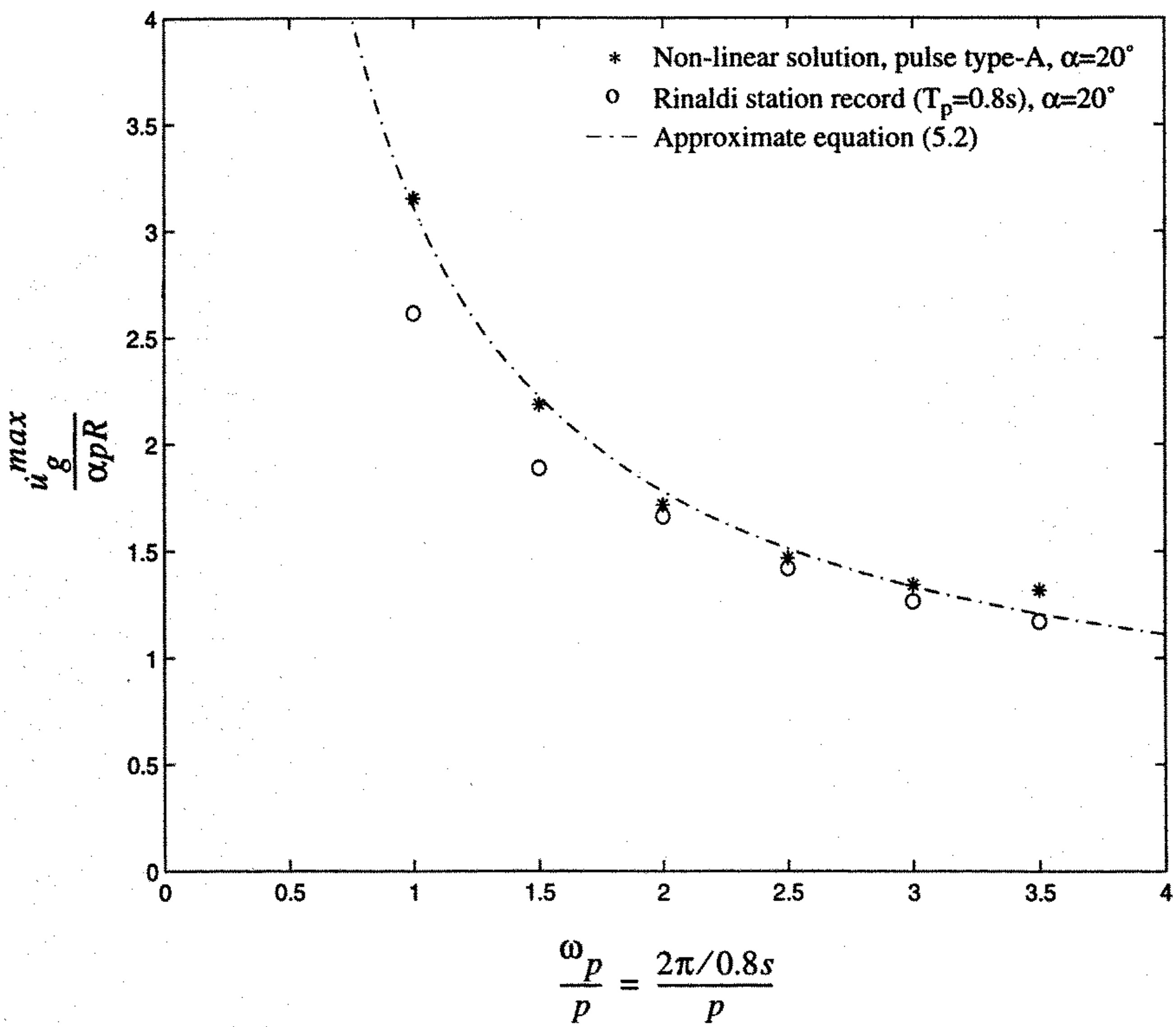

Figure 22: Spectrum of the minimum velocity amplitude of the Rinaldi station motion (circles) and a pulse type-A (stars) required to overturn a free standing block.

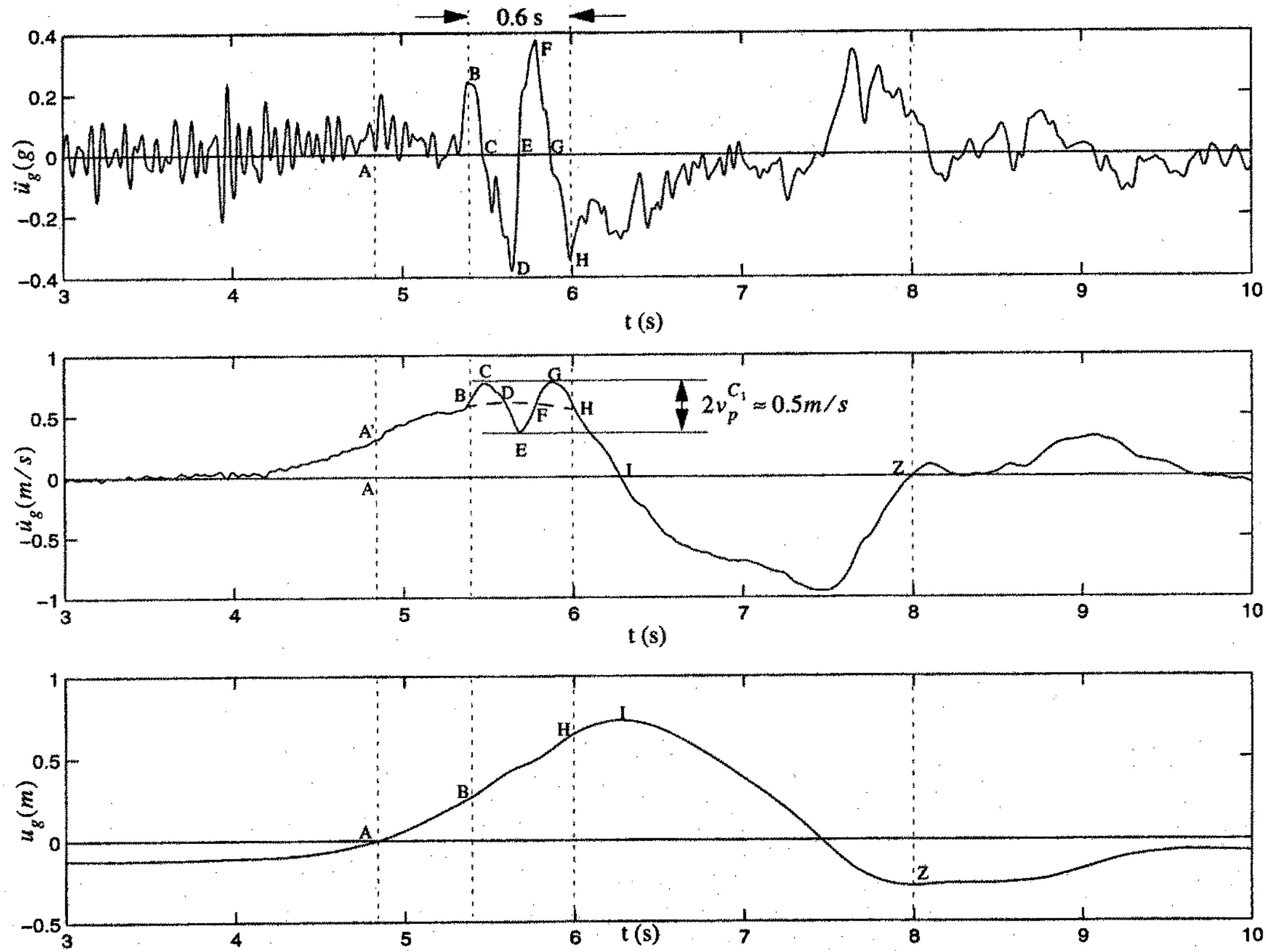

Figure 23: Zoom into the acceleration, velocity, and displacement histories recorded at the El Centro Array #5 station, during the October 15th, 1979 Imperial Valley, California earthquake

Consider now a set of geometrically similar blocks with slenderness α, and various sizes, R, subjected to the El Centro Array #5 acceleration shown in Figure 23. Within the limitations of the proposed approximate analysis, equation (7.1) indicates that any block with p such that

$$a_p^{C_1} \geq \alpha g\left(1 + \frac{1}{6}\frac{\omega_p^{C_1}}{p}\right) \tag{9.1}$$

will overturn due to the type C_1 pulse BCDEFGH. After rearranging terms equation (9.1) gives

$$p \geq \frac{\omega_p^{C_1}}{6(a_p^{C_1} - 1)} . \tag{9.2}$$

Accordingly, blocks which are small enough such that inequality (9.2) is satisfied will be overturned by the short duration type-C_1 pulse. Larger blocks will survive the type C_1 pulse BCDEFGH, and will be subjected to the long duration pulse AIZ. According to equation (6.1), any block with p such that

$$a_p^{B} \geq \alpha g\left(1 + \frac{1}{4}\frac{\omega_p^{B}}{p}\right) \tag{9.3}$$

will overturn due to the type-B pulse AIZ. Rearranging terms inequality (9.3) gives

$$p > \frac{\omega_p^{B}}{4\left(\dfrac{a_p^{B}}{\alpha g} - 1\right)} . \tag{9.4}$$

The substitution of

$$\omega_p^{C_1} = k\omega_p^{B} = k\omega_p , \;\; k > 1 , \tag{9.5}$$

and

$$a_p^{C_1} = \mu a_p^{B} = \mu a_p , \;\; \mu > 1 , \tag{9.6}$$

into equation (9.2) gives

$$\frac{\omega_p}{p} \le 6\frac{\left(\mu\frac{a_p}{\alpha g} - 1\right)}{k} \tag{9.7}$$

Consequently, blocks which are small enough to satisfy inequality (9.7) will overturn due to the short period type-C_1 pulse, whereas blocks of a size that satisfies

$$\frac{\omega_p}{p} \le 4\left(\frac{a_p}{\alpha g} - 1\right) \tag{9.8}$$

will overturn due to the long period type-B pulse. The cut-off frequency is the intersection of the two lines defined by (9.7) and (9.8) when the equality sign is considered. For example, for the El Centro Array #5 station record, $k \approx 6$ and $\mu \approx 2$. Figure 24 shows that blocks with ω_p/p less than 2 will overturn due to the short duration pulse, whereas blocks with $\omega_p/p > 2$ will overturn due to the long-duration type-B pulse. This calculation indicates that the 0.5m x 1.5 m block with p=2.157 rad/s will overturn due to the short type-C_1 pulse of the El Centro Array #5 record since $\omega_p = \omega_p^B = 2\pi/3.2$ rad/s and therefore $\omega_p/p = 0.91$, which is less than 2. Figure 25 (left) plots the rocking response of the 0.5m x 1.5m block subjected to 122% level of the El Centro Array #5 motion and the block does not overturn, whereas on the right, the block overturns for a slightly higher acceleration level. The block clearly overturns due to the presence of the short duration pulse. Figure 26 (top) plots the minimum overturning acceleration spectrum of the El Centro Array #5 record as a function of ω_p/p, where $\omega_p = 2\pi/3.2$ rad/s is the pulse frequency of the 3.2 second duration pulse. Indeed, the spectrum has a distinct jump at $\omega_p/p \approx 2$. This is because, for values of $\omega_p/p < 2$, blocks overturn due to the presence of the short-period type-C_1 pulse, whereas for values of $\omega_p/p > 2$ blocks overturn due to the long duration type-B pulse as was predicted by Figure 24.

Figure 26 (bottom) plots the minimum overturning velocity spectrum of the El Centro Array #5 record as a function of ω_p/p where $\omega_p = 2\pi/3.2$ rad/s. For values of $\omega_p/p > 2$, overturning of blocks occurs due to the 3.2 s duration type-B pulse of the record, and the overturing velocity spectrum correlates with the overturning velocity spectrum of a type-B pulse which is plotted

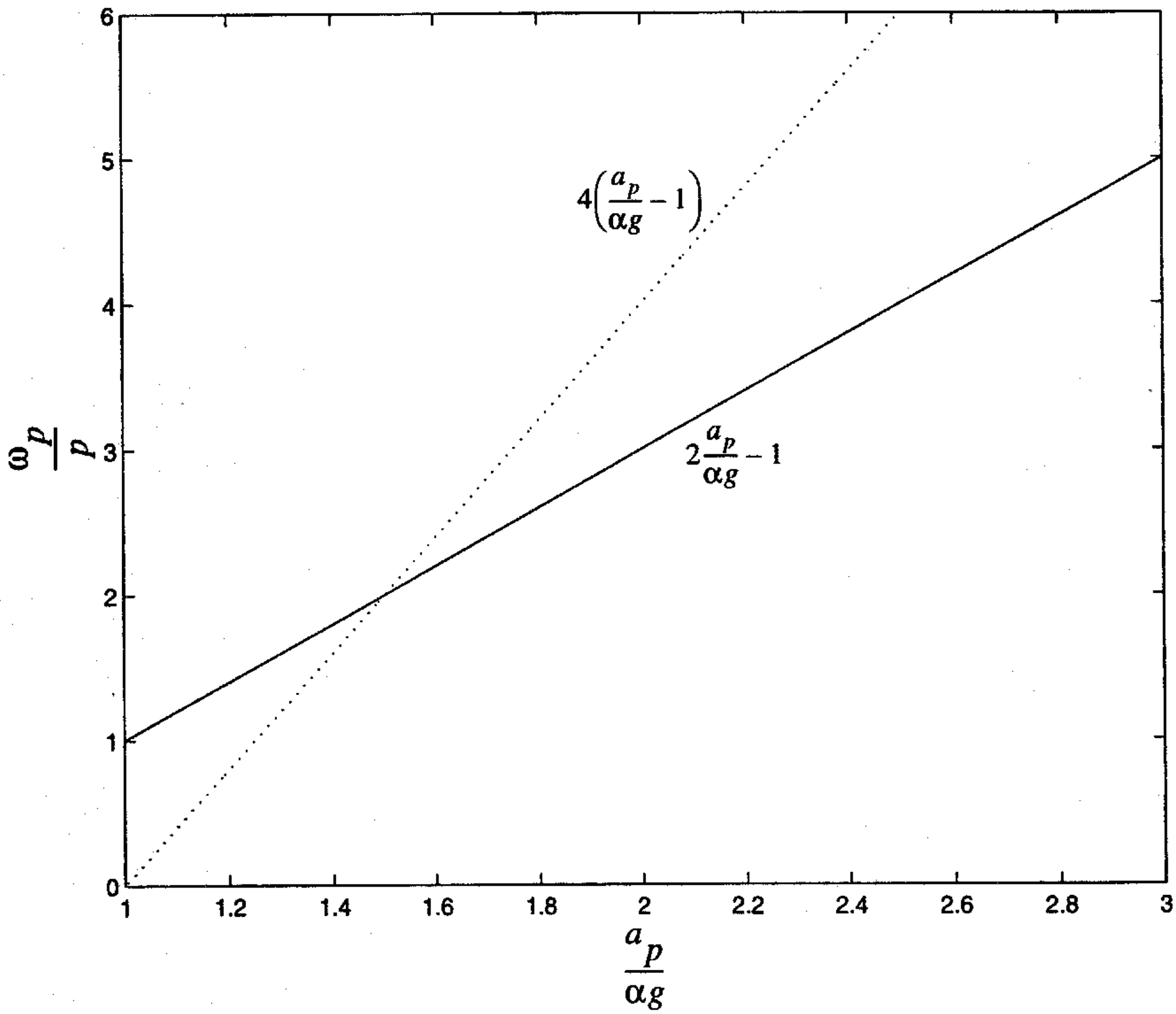

Figure 24: Boundaries of the overturning region on the acceleration-frequency plane.

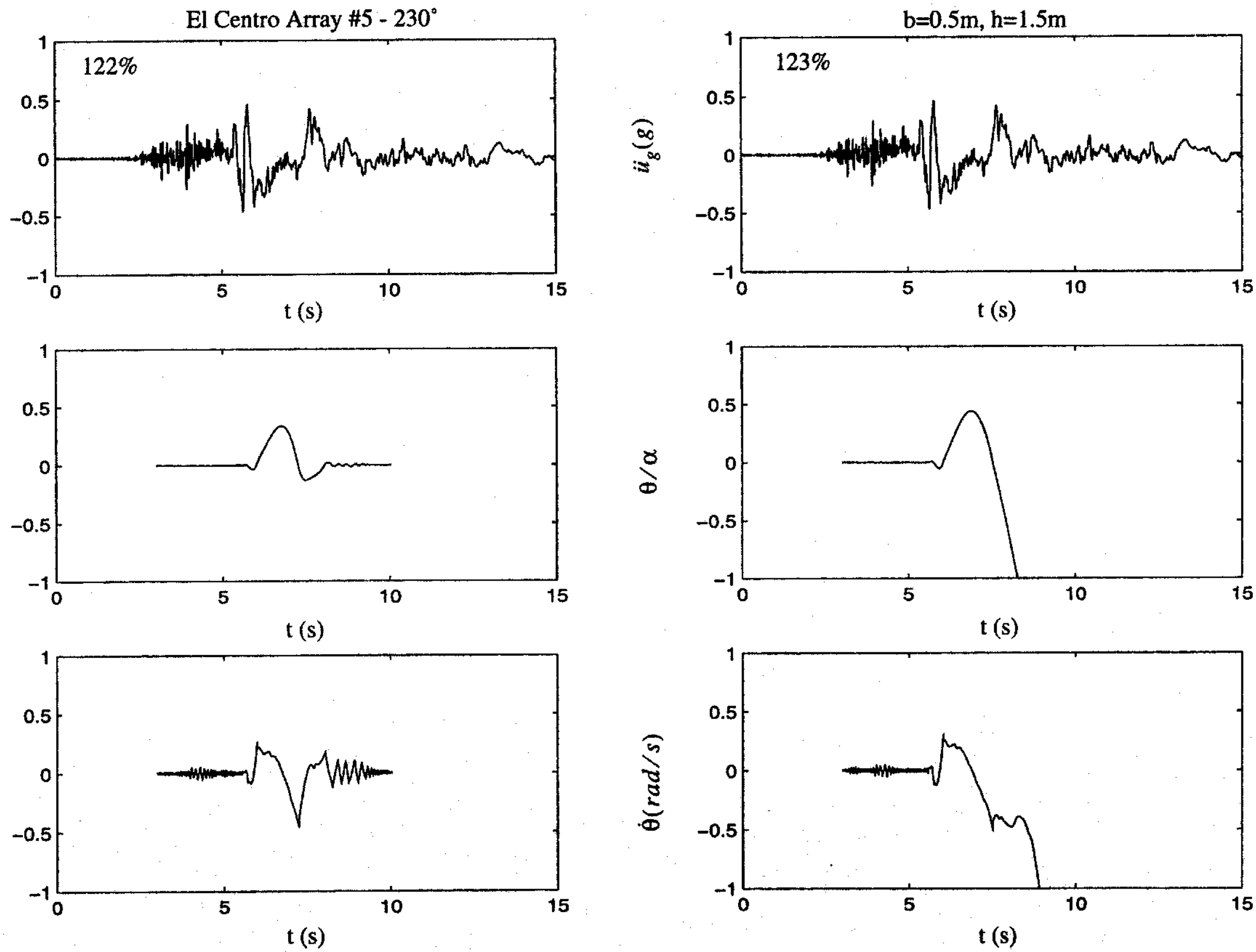

Figure 25: Rotation and angular velocity response time histories of a rigid block (b=0.5 m, h=1.5 m) subjected to the El Centro Array #5 motion. Left: no overturning (122% acceleration level). Right: overturning (123% acceleration level)

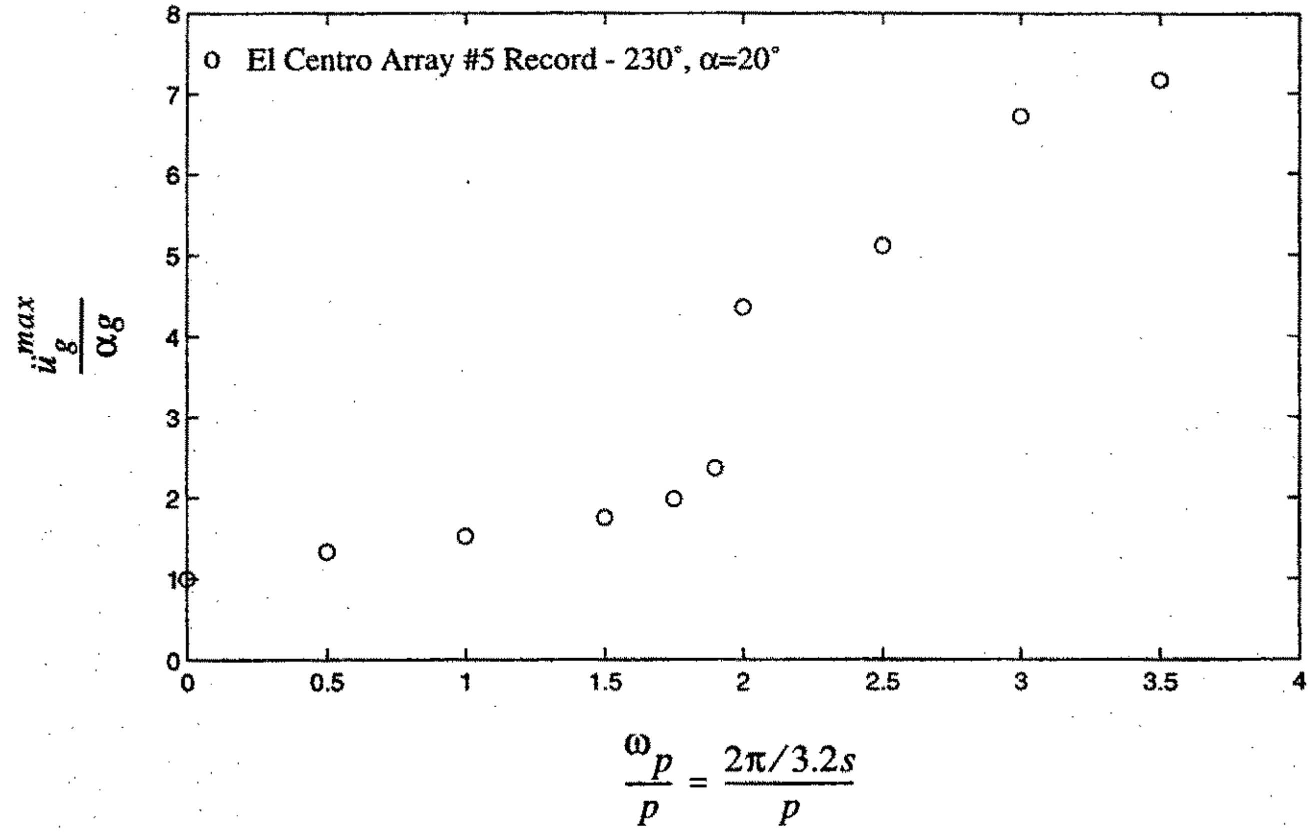

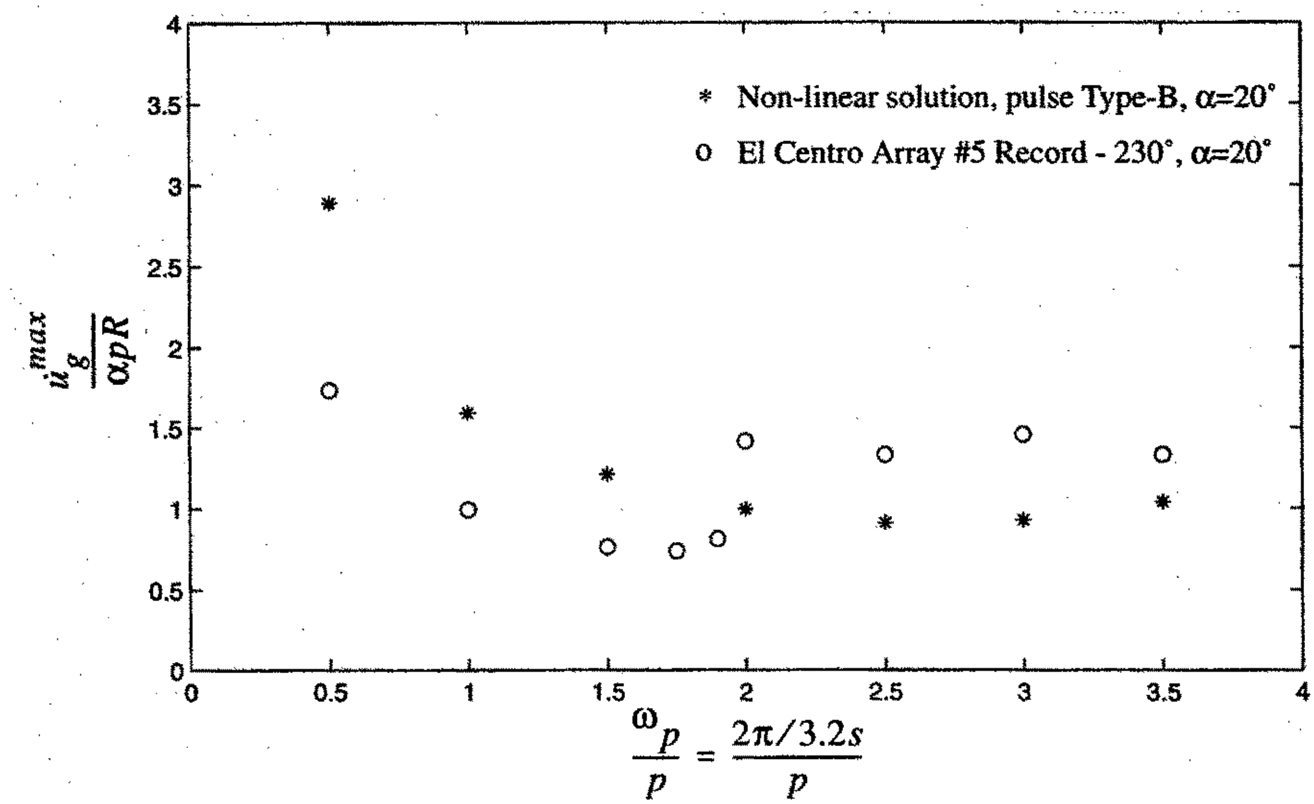

Figure 26: Spectrum of the minimum peak acceleration (top) and velocity (bottom) of the El Centro Array #5 motion needed to overturn a free standing block. The sudden jump near $\omega_p/p = 2$ indicates that smaller blocks ($\omega_p/p < 2$) overturn due to the presence of a pulse that is different from the pulse that overturns the larger blocks.

with stars. For values of $\omega_p/p < 2$ overturning of blocks occurs due to the 0.4 s duration type-C_1 pulse of the record This explains the lack of correlation between the circles and the stars for $\omega_p/p < 2$.

Figure 27 plots the first 10 seconds of the Sylmar station record shown in Figure 10. Because the ground displacement undergoes nearly 2.5 cycles, this motion was approximated with a type-C_2 pulse with period T_p=2.3s. Figure 27, however, shows that, just prior to the 4th second of the time history, there is a distinct fluctuation BCDEF that resembles a pulse type-B motion with duration $T_p^B = 0.42s$ $(\omega_p = 15 rad/s)$ and an acceleration amplitude, $a_p^B = \omega_p^B v_p^B \approx 0.50g$, which is three times the acceleration amplitude $a_p^{C_2} = \omega_p^{C_2} v_p^{C_2} \approx 0.17g$, of the long duration pulse, AIZ. Consider again a set of geometrically similar blocks with slenderness α and various sizes R, subjected to the Sylmar record. Within the limitations of the proposed approximate analysis, equation (6.1) indicates that any block with p that satisfies (9.4) will overturn due to the short duration type-B pulse BCDEF. Larger blocks will survive the type-B pulse, BCDEF, and will be subjected to the long duration type-C_2 pulse, AIZ. Blocks with p such that

$$p > \frac{\omega_p^{C_2}}{6\left(\frac{a_p^{C_2}}{\alpha g} - 1\right)} \tag{9.9}$$

will overturn due to this pulse.

The substitution of

$$\omega_p^B = k\omega_p^{C_2} = k\omega_p \tag{9.10}$$

and

$$a_p^B = \mu a_p^{C_2} = \mu a_p \tag{9.11}$$

into equation (9.4) gives

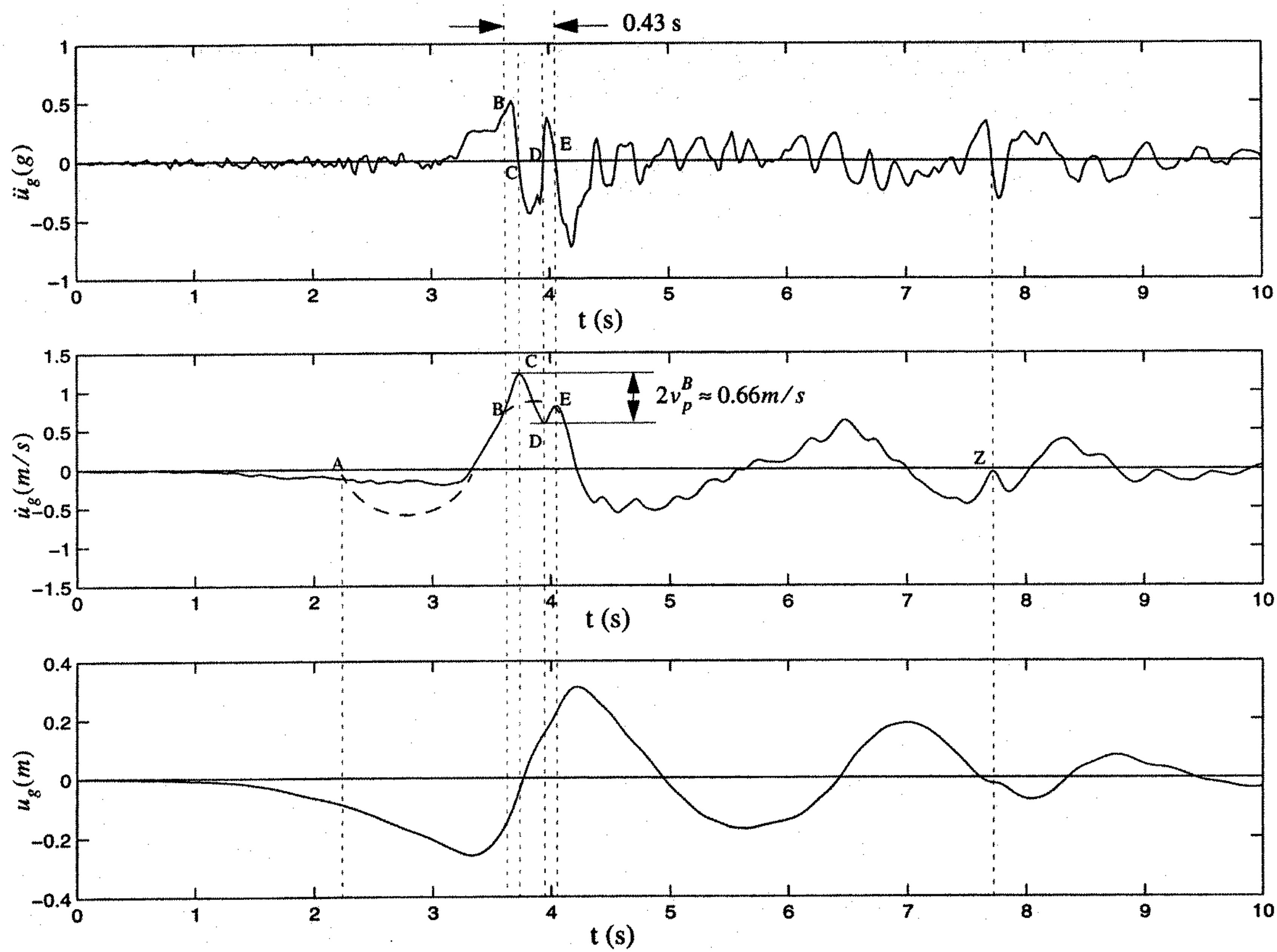

Figure 27: Zoom into the acceleration, velocity, and displacement histories recorded at the Sylmar station during the January 17th, 1994 Northridge, California earthquake.

$$\frac{\omega_p}{p} < \frac{4\left(\frac{\mu a_p}{\alpha g} - 1\right)}{k} \tag{9.12}$$

Consequently, blocks which are small enough that satisfy inequality (9.12) will overturn due to the short period type-B pulse, whereas blocks with sizes that satisfy the inverse of (9.2)

$$\frac{\omega_p}{p} < 6\left(\frac{a_p}{\alpha g} - 1\right) \tag{9.13}$$

will overturn due to the long period type-C pulse. The cut-off frequency is the intersection of the two lines defined by (9.12) and (9.13) when the equality sign is considered. For the Sylmar record, $k \approx 5.5$ and $\mu \approx 3$. Figure 28 shows that blocks with ω_p/p less than 2.2 will overturn due to the short duration type-B pules, whereas blocks with $\omega_p/p > 2.2$ will overturn due to the long duration type-C_2 pulse. As an example, from Figure 27 one concludes that the 0.5m x 1.5m block with p=2.157rad/s will overturn due to the short duration type-B pulse of the Sylmar record, since $\omega_p = \omega_p^{C_2} = 2\pi/2.3s = 0.87\pi$ rad/s and therefore $\omega_p/p = 1.27$, which is less than 2.2.

The approximate analysis presented herein is implemented to provide an estimate of the level of the Sylmar record that is needed to overturn the 0.5m x 1.5m block. In this case, where a short duration pulse overrides a longer duration pulse, the situation is more complex. For instance, the approximate equation (6.2) that provides the minimum overturning velocity cannot provide a dependable estimate since the block has most likely a non-zero velocity when the BCDE type-B pulse strikes. Accordingly, we can only use the approximate expressions for the overturning acceleration. The duration of the type-B pulse is $T_p^B = 0.43s$ $(\omega_p^B = 14.60)$, and therefore, for the 0.5m x 1.5m block (p=2.157), $\omega_p/p = 6.77$. Equation (6.1) indicates that the overturning acceleration of a type-B pulse is $a_{po}/\alpha g = 1 + (1/4)6.77 = 2.69$. On the other hand, the acceleration associated with the type-B pulse in the Sylmar record is $a_p/\alpha g = 0.50/0.3217 = 1.55$. Consequently, the estimated level of the Sylmar record that will overturn the 0.5m x 1.5m block is $2.69/1.55 \approx 1.77 = 177\%$.

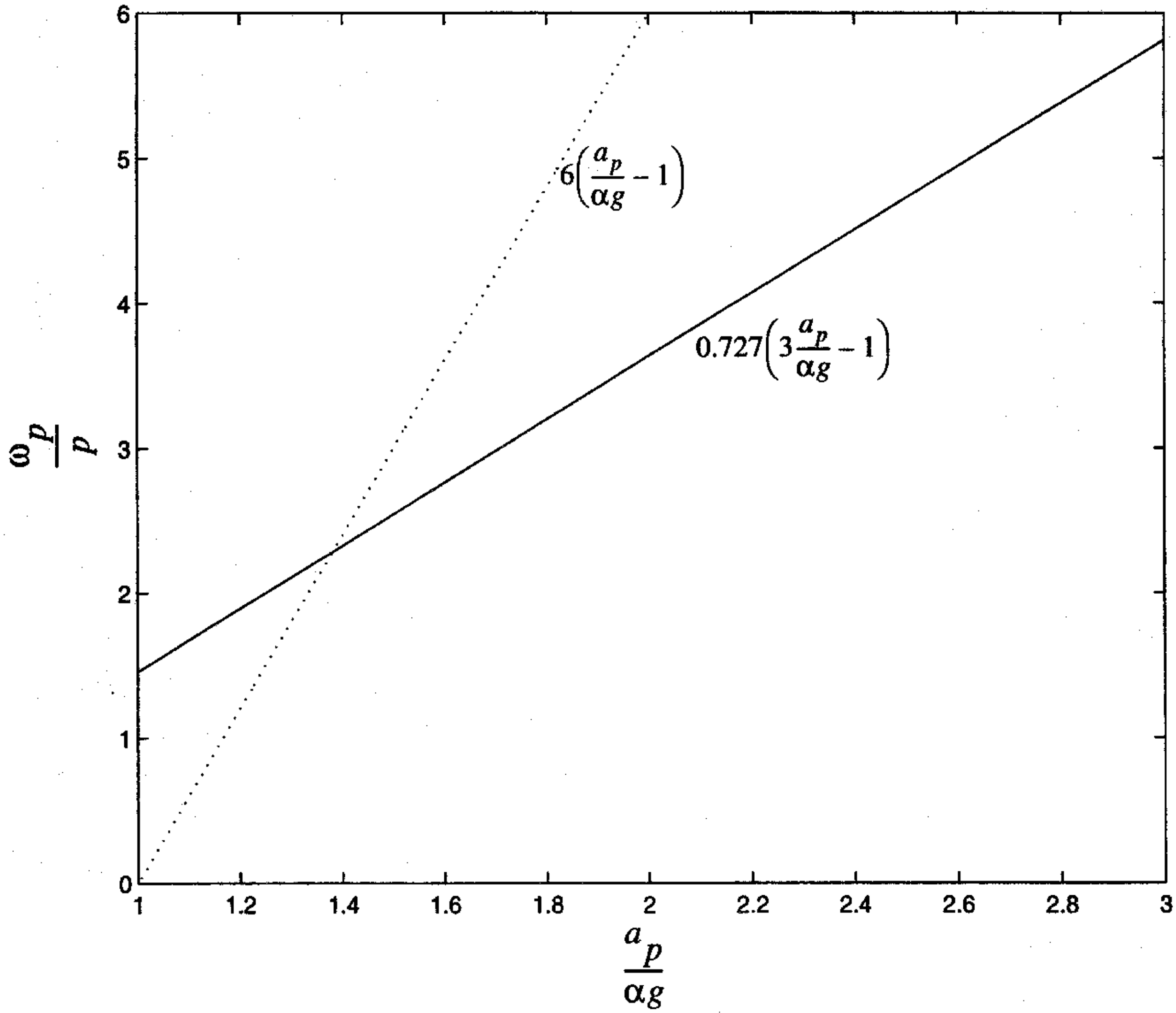

Figure 28: Boundaries of the overturning region on the acceleration-frequency plane.

Figure 29 (left) plots the rocking response of the 0.5m x 1.5m block subjected to 116% level of the Sylmar record and the block does not overturn, whereas on the right, the block overturns for a slightly higher acceleration level. The block clearly overturns due to the presence of the short duration type-B pulse. However, the level of the Sylmar record that is needed to overturn the block is only 117%, which is less than the 177% predicted with the approximate method. It is worth noting, however, that the rocking response of the block is strongly nonlinear since at 116% the maximum rotation of the block is less than half the critical value. Figure 30 (top) plots the minimum overturning acceleration spectrum of the Sylmar record as a function of ω_p/p, where $\omega_p = 0.87\pi$ is the pulse frequency of the 2.3 sec duration type-C_2 pulse. The spectrum has a distinct jump at $\omega_p/p = 2$, which is the value of the cut-off frequency predicted by Figure 28. Figure 30 (bottom) plots the minimum overturning velocity spectrum of the Sylmar record as a function of ω_p/p together with the velocity spectrum of a type-C_2 pulse (stars). The two spectra correlate for $\omega_p/p > 2.2$, since blocks with $\omega_p/p < 2.2$ overturn due to the type-B pulse and not the type-C_2 pulse. The foregoing analysis shows that the overturning of rigid blocks for strong ground motions is a problem with several scales. Small blocks overturn from small duration pulses with high accelerations. Larger blocks overturn from larger duration pulses that might have smaller acceleration values. The two foregoing examples illustrate that blocks as big as a typical transformer $(p \approx 2.1)$ overturn due to pulses that have substantially shorter duration than the duration of the main pulse that generates most of the ground velocity and ground displacements recorded near the source of strong ground motions.

The developed methodology is now used to estimate the level of the fault parallel component of the Lucerne Valley record shown in Figure 6 that is needed to overturn the 0.5m x1.5m block (p=2.157, α=0.3217). Figure 31 zooms into the Lucerne Valley motion between 5 secs and 15 secs. On top of the 7.0 sec duration forward pulse (AZ) one can distinguish a type-C_2 pulse that crosses the AZ forward pulse at points BCDEFG. This type-C_2 pulse has an approximate period of $T_p^{C_2} \approx 1.14s$ and a velocity amplitude of $v_p^{C_2} \approx 0.18m/s$. The peak ground acceleration of the Lucerne Valley record occurs at $t \approx 11.5s$. This sharp spike is due to a short type-B pulse with

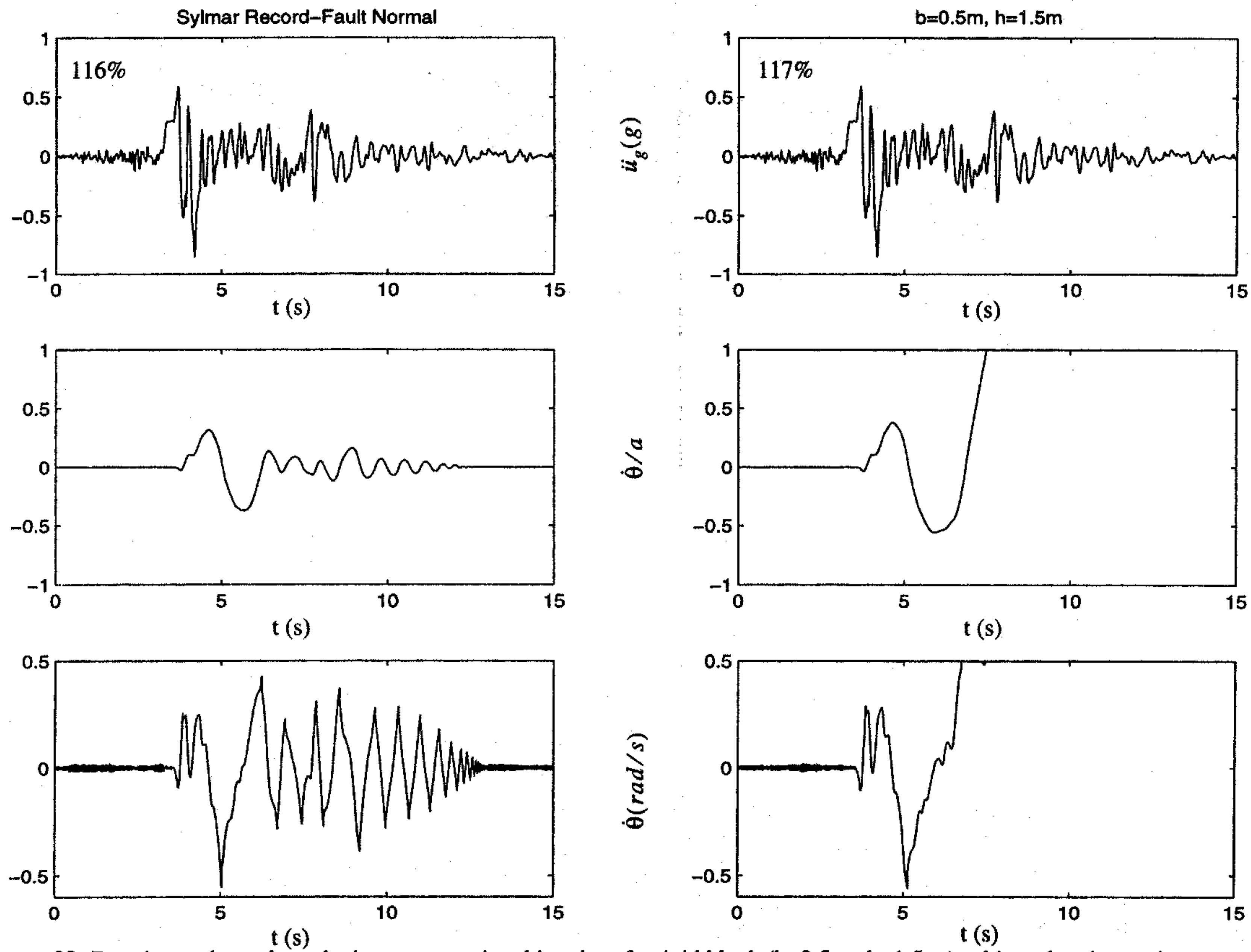

Figure 29: Rotation and angular velocity response time histories of a rigid block (b=0.5 m, h=1.5 m) subjected to the motion recorded at the Sylmar station. Left: no overturning (116% acceleration level). Right: overturning (117% acceleration level).

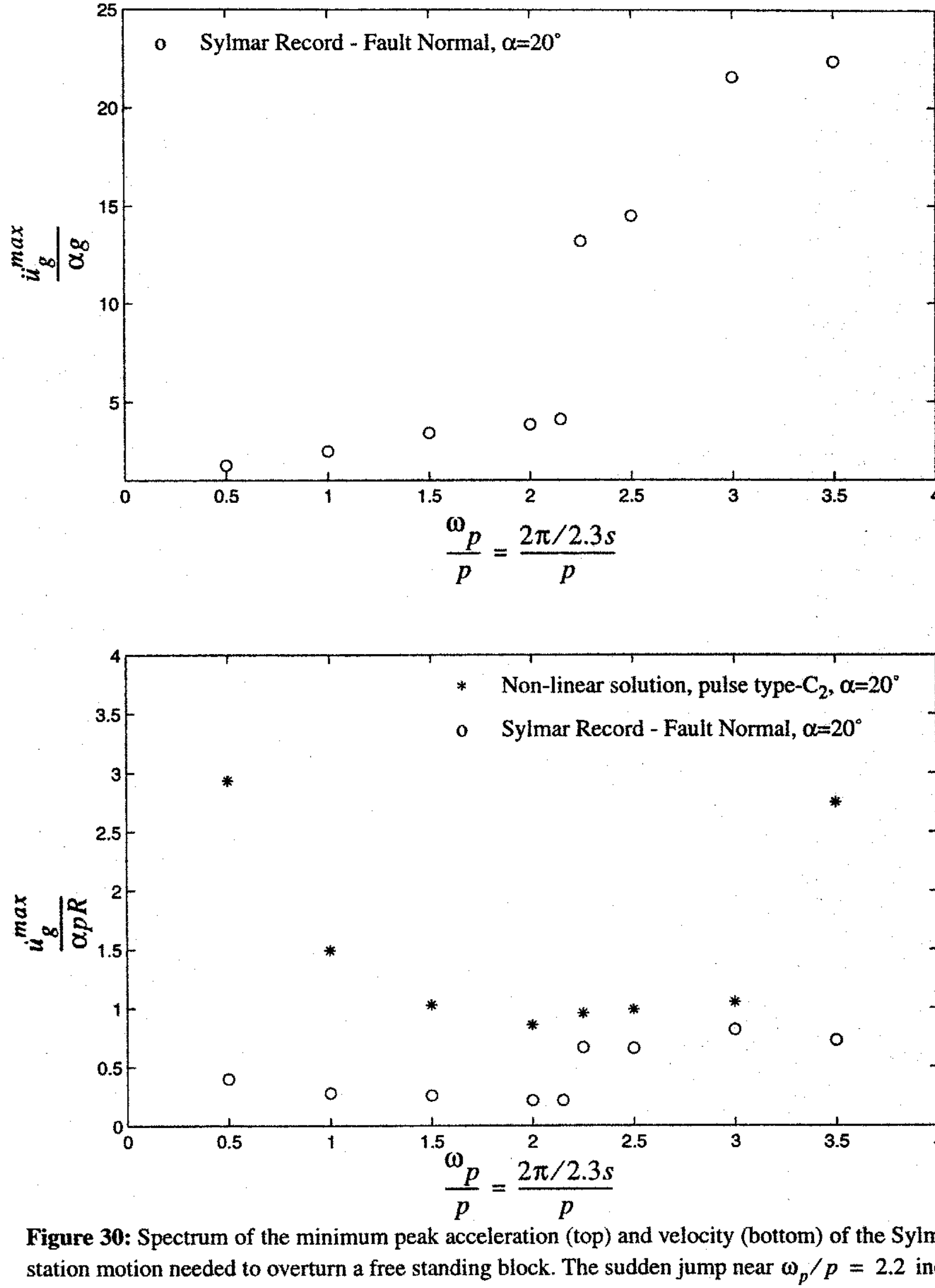

Figure 30: Spectrum of the minimum peak acceleration (top) and velocity (bottom) of the Sylmar station motion needed to overturn a free standing block. The sudden jump near $\omega_p/p = 2.2$ indicates that smaller blocks ($\omega_p/p < 2.2$) overturn due to the presence of a pulse that is different from the pulse that overturns the larger blocks.

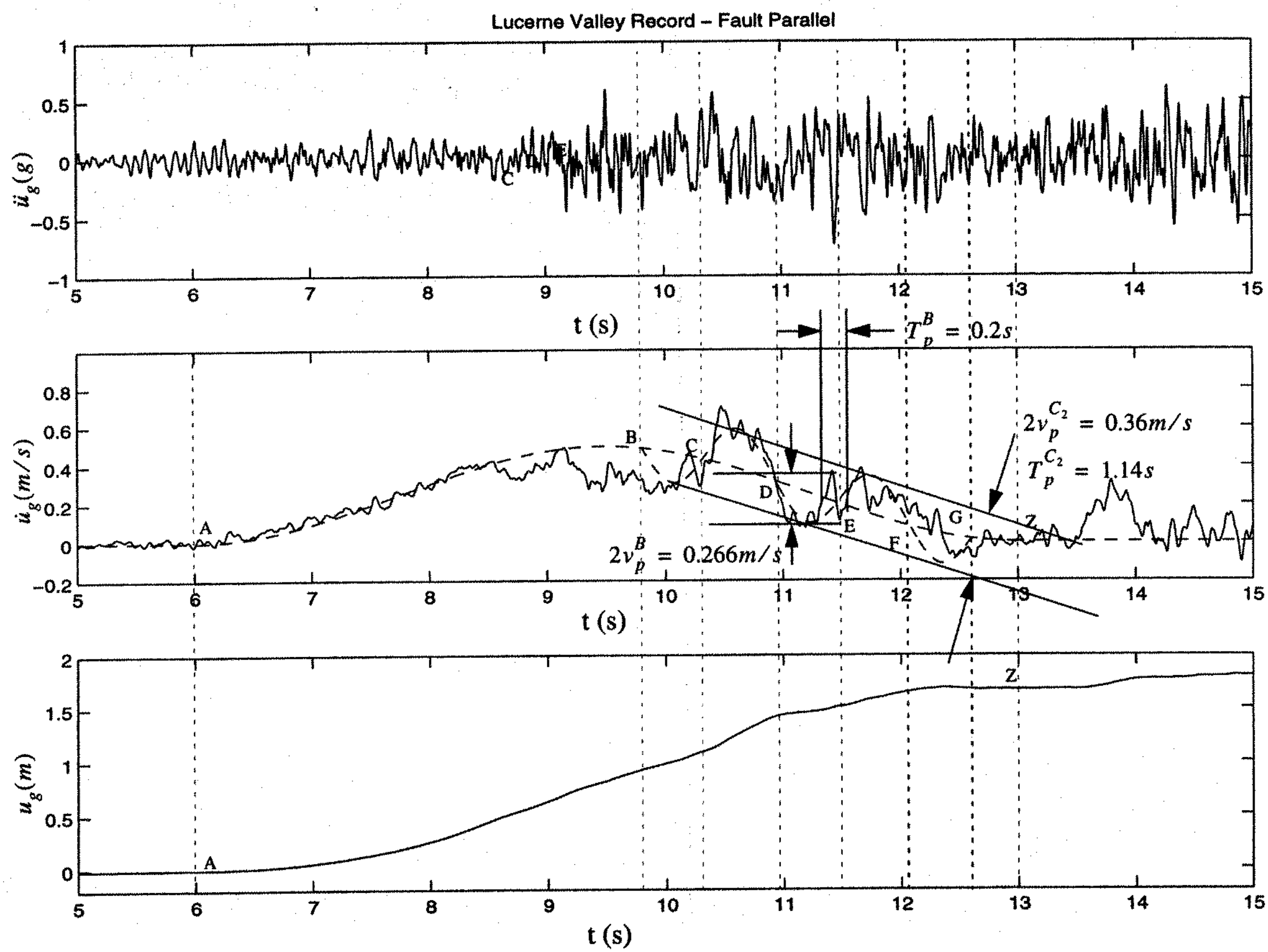

Figure 31: Zoom into the acceleration, velocity, and displacement histories recorded at the Lucerne Valley station during the June 28th, 1992 Landers, California earthquake.

duration $T_p^B \approx 0.2s$. The characteristics of these three pulses together with the values of their minimum overturning acceleration amplitudes, a_{po} , that were computed with equations (5.1), (6.1), and (7.1) are summarized in Table 9.1. According to the approximate equations (5.1), (6.1), and (7.1), the 0.5m x 1.5m block will overturn due to the long type-A pulse when subjected to 15 times its level; it will overturn due to the medium type-C_2 pulse when subjected to 4.5 its level; and it will overturn due to the short type-B pulse when subjected to 2.99 times its level.

TABLE 9.1. Characteristics of three distinct pulses of the Lucerne Valley record and their levels needed to overturn the 0.5m x 1.5m block (p=2.157, α=0.3217)

Pulse Type\ Pulse Characteristic	Long Pulse Type-A	Medium Pulse Type-C_2	Short Pulse Type-B
$v_p(m/s)$	0.50	0.18	0.133
$T_p(s)$	7.0	1.14	0.20
$\omega_p(rad/s)$	0.90	5.51	31.41
$a_p(g)$	0.032	0.101	0.500
ω_p/p	0.417	2.555	14.56
$a_p/\alpha g$	0.071	0.314	1.55
$a_{po}/\alpha g$	$1+\frac{1}{6}\frac{\omega_p}{p}$ =1.07	$1+\frac{1}{6}\frac{\omega_p}{p}$ =1.426	$1+\frac{1}{4}\frac{\omega_p}{p}$ =4.64
a_{po}/a_p	15	4.5	2.99

Figure 32 shows that the 0.5m x 1.5 m block that resembles the size of an electrical transformer (see Table 2.1) overturns at a 2.74 level of the Lucerne Valley record, a value that is remarkably close to the 2.99 level that was computed with hand calculations.

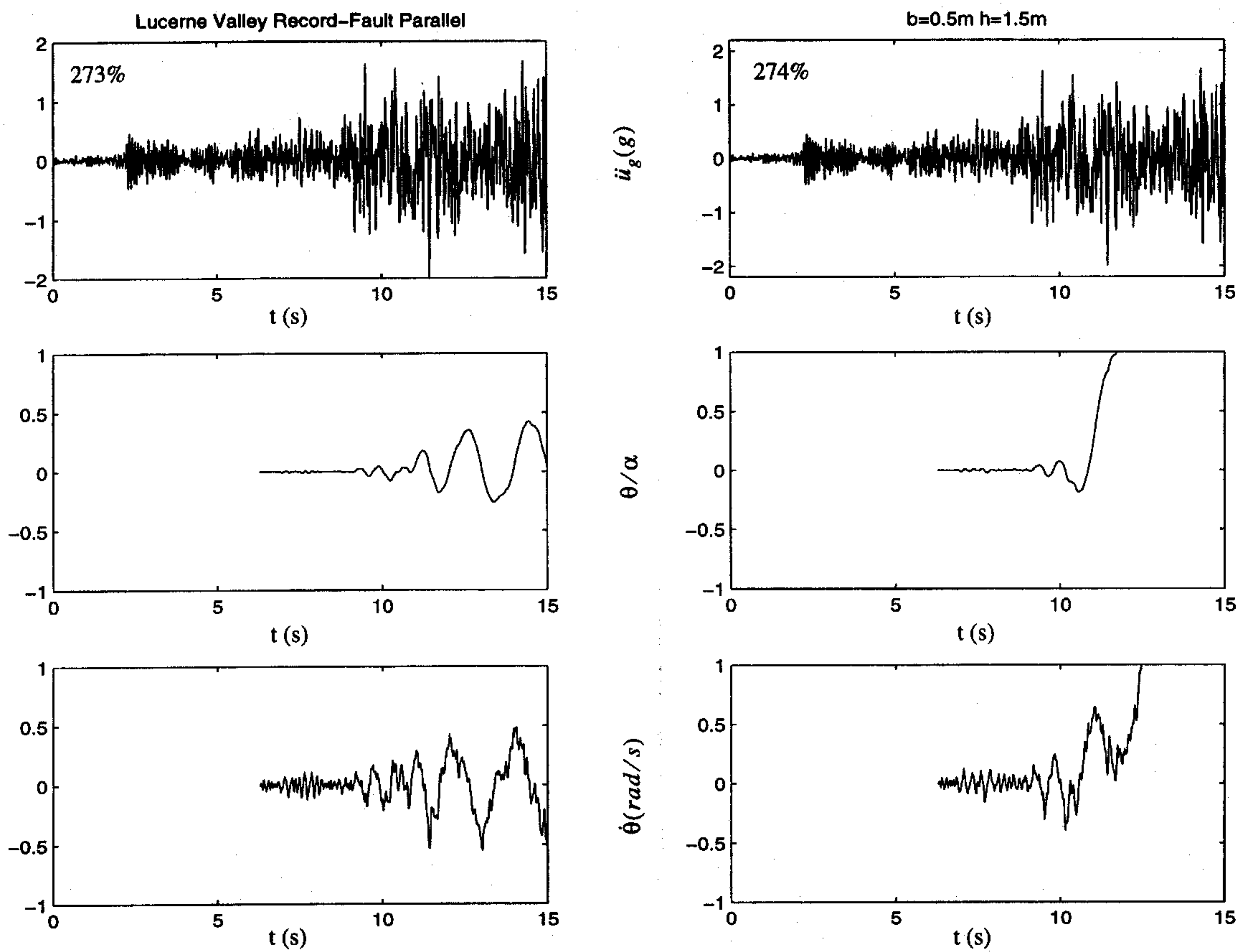

Figure 32: Rotation and angular velocity histories of a rigid block (b=0.5m, h=1.5m) subjected to the motion recorded at the Lucerne Valley station. Left: no overturning (273% acceleration level). Right: overturning (274% acceleration level).

9.1 Outline of the Proposed Procedure

The outline of the proposed procedure to estimate the level of a given ground motion that is needed to overturn a piece of electrical equipment, with a given slenderness, α, and frequency parameter, p, is offered below:

1. Locate the time, in the record, of the peak ground acceleration, a_p. For instance, in the Lucerne Valley record, shown in Figure 31, the maximum acceleration, a_p, occurs at approximately t=11.5 s.
2. Zoom into the velocity record near the time of the peak ground acceleration, a_p, and identify the type and period, T_p, of the local pulse that results into the peak ground acceleration. Estimate the velocity amplitude, v_p, of the local pulse. The estimated values of T_p and v_p should satisfy $a_p \approx \omega_p v_p = \frac{2\pi}{T_p} v_p$ (for instance, in the Lucerne Valley record, shown in Figure 31, the local pulse is of type-B, and its period is approximately $T_p^B \approx 0.2s$).
3. Compute the minimum overturning acceleration $a_{po} = \alpha g[1 + \beta(\omega_p / p)]$ where $\beta = 1/6$ for type A or C_n pulses, and $\beta = 1/4$ for a type B pulse.
4. Compute the ratio a_{po}/a_p. This ratio gives the approximate level of the ground motion that will overturn a block with slenderness α and frequency parameter p. In the Lucerne Valley record shown in Figure 31 $a_{po}/a_p = 2.99$.
5. In case that the velocity or displacement history exhibit a distinguishable long duration pulse, identify the velocity amplitude, v_p, and the duration T_p, of this pulse. Then, compute the corresponding acceleration of this pulse as $a_p = \frac{2\pi}{T_p} v_p = \omega_p v_p$.
6. Compute the minimum overturning acceleration, a_{po}, of this pulse as in step 3.
7. Repeat step 4 using the value a_p estimated in step 5 and the value of a_{po} computed in step 6. If the ratio a_{po}/a_p that was computed in step 7 is larger than the ratio computed in step 4, the block overturns due to the short duration pulse for the level of the ground motion computed in step 4. In contrast, if the ratio a_{po}/a_p computed in step 7 is smaller than the one computed in step 4, the block overturns due to the long duration pulse and for the level of the ground motion computed in step 7.

This study indicates that electrical transformers with approximate values of slenderness α, and frequency parameter p, like those shown in Table 2.1, will most likely overturn due to the short duration pulse. Accordingly, only steps 1 through 4 are needed to estimate the level of the ground motion that will overturn a typical electrical transformer. Only very large objects, such as nuclear heat-exchange boilers, that their frequency parameter value is less than one $(p \leq 1)$, may overturn due to the presence of the long duration pulses. Thus, steps 5 to 7 should also be included in the procedure.

CHAPTER 10
CONCLUSIONS

The transient rocking response of electrical transformers subjected to horizontal trigonometric pulses and near source ground motion has been investigated in depth. First it was shown that the solution presented by Housner (1963) for the minimum acceleration amplitude of a half-sine pulse that is needed to overturn a rigid block is unconservative. In reality, under a half-sine pulse a block overturns during its free-vibration regime and not at the instant that the pulse expires. Within the limits of the linear approximation, the correct expression that yields the minimum acceleration required to overturn a block was derived.

Physically realizable trigonometric pulses have been introduced, and their resemblance to select recorded near-source ground motions was illustrated. The overturning potential of forward pulses, forward-and-back pulses, and pulses that result in displacement histories with one or two main cycles was examined. Under horizontal excitation, the three parameters that control overturning are the normalized pulse acceleration $a_p/\alpha g$, the frequency ratio ω_p/p, and the slenderness α. It was found that, at the low frequency limit $(\omega_p/p < 3)$, the normalized overturning acceleration amplitude of the pulse, $a_{po}/\alpha g$, is larger than one and increases linearly with ω_p/p. For values of $\omega_p/p > 3$, the normalized overturning acceleration amplitude increases non-linearly with ω_p/p, exhibiting a stiffening effect. Accordingly, the static solution (West's formula) is increasingly over-conservative as ω_p/p increases.

The toppling of smaller blocks is more sensitive to the peak ground acceleration, whereas the toppling of larger blocks depends on the incremental ground velocity. A simple method that involves hand calculations was developed to estimate the level of a recorded ground motion that is needed to overturn a given block. It was found that blocks as big as typical electric transformers $(p \approx 2)$ overturn due to short-duration, high-acceleration pulses that often override the main long-duration pulse that generates most of the ground velocity and ground displacement recorded near the source of strong ground motions. Accordingly, near source ground motions do not bear any exceptional overturning potential for electrical transformers. In contrast, larger objects such as nuclear heat-exchange boilers $(p \approx 1)$ will overturn due to the long duration pulse. For these larger objects, long-period ground motions might be particularly destructive.

Under realistic conditions, the rocking response of a rigid block is affected by additional factors such as the vertical component of the ground acceleration and the additional energy loss due to plastic deformations at the pivot points. The effects of these factors are the subject of a future study. This study shows that the overturning potential of a recorded ground motion depends both on the duration and the acceleration level of its pulses.

The presented approximate method, although restricted to horizontal seismic excitations, elucidates the rocking response of electrical equipment which is found to be quite ordered and predictable.

REFERENCES

J. C. Anderson and V. Bertero, “Uncertainties in establishing design earthquakes”, *Journal of Struct. Eng.*, ASCE, Vol. 113, 1709-1724, (1986).

J. G. Anderson, P. Bodin, J. N. Brune, J. Prince, S. K. Singh, R. Quaas and M. Onate, “Strong ground motion from the Michoagan, Mexico, earthquake”, *Science*, Vol. 233, 1043-1049, (1986).

M. Aslam, W. G. Godden and D. T. Scalise, “Earthquake rocking response of rigid bodies”, *Journ. Engrg. Mech. Div.* ASCE 106, 377-392, (1980).

M. Campillo, J. C. Gariel, K. Aki and F. J. Sanchez-Sesma, “Destructive strong ground motion in Mexico City: Source, path and site effects during the great 1985 Michoagan earthquake”, *Bull. Seism. Soc. Am.*, Vol. 79, No 6, 1718-1735, (1989).

E. Fujisaki, Personal communication, (1998).

S. J. Hogan, “On the dynamics of rigid-block motion under harmonic forcing”, *Proc. R. Soc. London*, A425, 441-476, (1989).

S. J. Hogan, “The many steady state responses of a rigid block under harmonic forcing”, *Earthquake Eng. and Str. Dynamics*, Vol. 19, 1057-1071, (1990).

G. W. Housner, “The behavior of inverted pendulum structures during Earthquakes”, *Bull. Seism. Soc. Am.,* Vol. 53, 404-417, (1963)

W. D. Iwan and X. D. Chen, “Important near-field ground motion data from the Landers earthquake”, *Proc. 10th European Conf. Earthquake Engrg.*, Vienna, 1994.

L. S. Jaycobsen and R. S. Ayre, *Engineering Vibrations*, McGraw-Hill, New York, NY, 1958.

N. Makris, “Rigidity-Plasticity-Viscocity: Can Electrorheological dampers protect base-isolated structures from near-source ground motions?”, *Earthq. Eng. and Struct. Dynamics*, Vol. 26, 571-591, (1997).

MATLAB, *High performance numeric computation and visualization software*, The MathWorks Inc., (1982).

J. Milne, “Seismic experiments”, *Trans. Seism. Soc. Japan*, 8, 1-82, (1885).

A. Pompei, A. Scalia and M. A. Sumbatyan, “Dynamics of rigid block due to horizontal ground motion”, *Journal of Engineering Mechanics*, ASCE, Vol. 124, 713-717, (1998).

A. Scalia and M. A. Sumbatyan, “Slide rotation of rigid bodies subjected to a horizontal ground motion”, *Earthquake Eng. and Str. Dynamics*, Vol. 25, 1139-1149, (1996).

C. Sim, A. K. Chopra and J. Penzien, “Rocking response of rigid blocks to earthquakes”, *Earthquake Engineering and Structural Dynamics*, Vol. 8, 565-587, (1980)

P. D. Spanos and A. S. Koh, “Rocking of rigid blocks due to harmonic shaking”, *Journ. Engrg. Mech. Div.* ASCE 110, 1627-1642, (1984).

W. K. Tso and C. M. Wong, “Steady state rocking response of rigid blocks Part 1: Analysis”, *Earthq. Eng. Struct. Dynamics*, Vol. 18, 89-106, (1989 a).

W. K. Tso and C. M. Wong, “Steady state rocking response of rigid blocks Part 2: Experiment”, *Earthq. Eng. Struct. Dynamics*, Vol. 18, 107-120, (1989 b).

Z. Y. Zhu and T. T. Soong, “Toppling fragility of unrestrained equipment”, *Applied Technology Council*, ATC-29-1, (1997).